

Assessing the effects of restoration and conservation on gaseous carbon fluxes and climate mitigation capacity across six European coastal wetlands

Miguel Cabrera-Brufau^{*a}, Camille Minaudo^a, Katrin Attermeyer^b, Alba Camacho-Santamans^a, Rafael Carballeira^c, Benjamin Misteli^b, Jorge Montes-Pérez^a, Daniel Morant^c, Biel Obrador^a, Antonio Picazo^c, Carlos Rochera^c, Mihai Adamescu^d, Raquel Ambrosio^e, Giancarlo Bachi^f, Nina Bègue^e, Martynas Bučas^g, Lídia Cañas Ramírez^a, Marco Carloni^f, Lamara Cavalcante^h, Constantin Cazacu^d, Giovanni Checcucci^f, J. Pedro Coelho^h, Valentin Dinu^d, Valtere Evangelista^f, Ilenia Férez Martín^a, Jonas Gintauskas^g, Relu Giuca^d, Anis Guelmami^e, Mirco Guerrazzi^f, Samuel Hilaire^e, Marija Kataržytė^g, Ana I. Lillebø^h, Raquel Lizán^c, Bruna R.F. Oliveira^h, Vitor H. Oliveira^h, Marta Pedrón^c, Jolita Petkuvienė^g, Tudor Racoviceanu^d, Michael Ronse^e, Chiara Santinelli^f, Ana I. Sousa^h, Wouter Suykerbuykⁱ, Edvinas Tiškus^g, Claudia Tropea^f, Diana Vaičiūtė^g, Silvia Valsecchi^f, Marinka van Puijenbroekⁱ, Mourine J. Yegon^b, Antonio Camacho^{ct}, Daniel von Schiller^{at}

^a Departament de Biologia Evolutiva, Ecologia i Ciències Ambientals, Universitat de Barcelona, Av. Diagonal 643, 8028, Barcelona, Spain

^bWasserCluster Lunz - Biologische Station, University of Vienna, Dr. Carl Kupelwieser Promenade 5, 3293, Lunz am See, Austria

^cInstitut Cavanilles de Biodiversitat i Biologia Evolutiva, Universitat de València,
C/Catedràtic José Beltrán 2. 46980. Paterna. Spain

^d Department of Systems Ecology and Sustainability, University of Bucharest, spl. Independentei 91 - 95, 50095, Bucharest, Romania

⁹Institut de recherche pour la conservation des zones humides méditerranéennes, Tel Aviv, Israël.

Valat Le Sambuc, 13200 Arles, France

[†]Istituto di Biofisica, Consiglio Nazionale delle Ricerche (CNR) Pisa, Via Giuseppe Moruzzi 1, 56124 Pisa, Italy

¹ 30124, Pisa, Italy
² Marine Research Institute, Kleinéda University, Universitatea ave. 17, 93294, Kleinéda

- Marine Research II

Lithuanian

^h ECOMARE, CESAM - Centre for Environmental and Marine Studies, Department of Biology, University of Aveiro, Portugal. E-mail: carol@ua.pt

¹Wageningen Marine Research, Wageningen University & Research, Korringaweg 7, 4401

NT, Yerseke, The Netherlands

*Corresponding author, email: miguelcabrera@ub.edu

39 to the [Ecological Engineering](#) for peer review on 15/01/2026.

40 **Abstract**

41 Coastal wetlands play a substantial role in regulating Earth's climate through exchanges of
42 greenhouse gases (GHGs). Current European policies promote widespread coastal wetland
43 restoration to reverse historical losses and ongoing pressures. However, substantial
44 uncertainty remains regarding how CO₂ and CH₄ fluxes respond to restoration across
45 different coastal wetland types and whether these responses translate into net climate
46 mitigation in terms of CO₂ equivalents (CO₂-eq). We measured simultaneous CO₂ and CH₄
47 fluxes using static chambers across four seasons at multiple locations spanning preserved,
48 altered and restored sites within each of six European coastal wetlands of different
49 ecological types. By comparing GHG exchanges and resulting CO₂-eq balances across
50 wetlands, we identified the dominant biogeochemical drivers of CO₂ and CH₄ dynamics and
51 assessed the climate mitigation potential of conservation and restoration actions. CO₂
52 fluxes were primarily controlled by landscape-scale vegetation cover and inundation,
53 whereas CH₄ emissions responded to more subtle changes in water quality, salinity and
54 wetland hydrodynamics. Comparisons of CO₂-eq balances between altered and restored
55 sites revealed that seagrass replantation and eutrophication reversal generated significant
56 mitigation benefits, driven by enhanced CO₂ uptake and reduced CH₄ emissions,
57 respectively. In contrast, other restoration measures modified CO₂ and CH₄ fluxes in
58 opposing directions, resulting in non-significant net climatic effects of CO₂-eq balances.
59 Overall, our results demonstrate that climate mitigation outcomes of coastal wetland
60 restoration are both GHG-specific and wetland-type dependent, underscoring the need for
61 tailored restoration strategies and robust, multi-GHG monitoring to detect and accurately
62 quantify potential climatic benefits.

63 **Keywords:** coastal wetlands, ecological restoration, CO₂ fluxes, CH₄ fluxes, climate change
64 mitigation

65 1. Introduction

66 Coastal wetlands are relevant components of the global carbon (C) cycle and are widely
67 recognized as blue carbon ecosystems. Despite their relatively low areal extent, they exert
68 a disproportionate influence on the global climate by providing long-term C-sequestration
69 and regulating atmospheric greenhouse gas (GHG) concentrations (Mitsch et al., 2012).
70 Wetlands in good conservation status are highly productive ecosystems, where low oxygen
71 availability limits aerobic organic matter degradation, resulting in net uptake of carbon
72 dioxide (CO₂) and sequestration of C in sediments and biomass (Reddy et al., 2022). At the
73 same time, wetland anoxic sediments act as hot spots for methane (CH₄) emissions,
74 making up 20-30% of global CH₄ emissions (Saunois et al., 2016), particularly when they
75 are degraded by alterations enriching the organic content such as eutrophication (Morant
76 et al., 2020a, 2020b). While the magnitude of CO₂ exchanges typically exceeds that of CH₄,
77 the higher global warming potential of the latter has the potential to overcome the effects
78 of CO₂ uptake and might result in a net balance that favors atmospheric warming (Canadell
79 and Monteiro, 2023). Ultimately, the net radiative forcing of coastal wetlands is largely
80 determined by the net balance of CO₂ and CH₄ exchanges with the atmosphere.

81 Diverse historical and current pressures have led to important reductions of the extent and
82 quality of global wetland ecosystems (Fluet-Chouinard et al., 2023). While areal loss
83 quantification remains challenging, especially when assessing coastal zones with high
84 historical development and land-reclamation practices, estimates of European coastal
85 wetland loss exceed 65% during the last century (Airoldi and Beck, 2007). Further, the
86 majority of remaining European wetlands have a poor or bad ecological status (European
87 Environment Agency, 2024) and experience diverse natural and anthropogenic pressures
88 (Maes et al., 2020). Although conservation policies, such as those under Ramsar (Ramsar
89 Convention, 1971) and the UE habitats Directive, help preserve the remaining wetlands,
90 their historical losses mean that widespread restoration is still needed. In this context, the
91 recent EU Nature Restoration Regulation aims at reverting this widespread degradation and
92 recovering crucial ecosystems services lost (European Union, 2024). Among the potential
93 benefits of restoration, climate change mitigation is increasingly being used as a supporting
94 argument. However, large uncertainties remain on the climatic mitigation capacity of
95 coastal wetland restoration (Jones et al., 2024).

96 Coastal wetlands influence climate primarily through CO₂ and CH₄ exchange, governed by
97 the balance among photosynthesis, aerobic and anaerobic respirations releasing CO₂, as
98 well as methanogenesis (Reddy et al., 2022). While local climate and wetland type shape
99 baseline GHG fluxes (Camacho et al., 2017), ecosystem alteration and restoration can
100 modify these fluxes by changing key controls, including vegetation, nutrient inputs,
101 hydrology, salinity, and sediment redox conditions (Camacho-Santamans et al., 2025;
102 Morant et al., 2024). The biomass and type of dominant primary producers exert a large
103 impact on the primary productivity of wetlands, as they represent the basic functional
104 standing stock for photosynthetic CO₂ uptake. While nutrients are essential to maintain
105 plant photosynthetic rates, excessive nutrient loads, namely nitrogen and phosphorus, can
106 lead to eutrophication and uncontrolled proliferation of benthic algae and phytoplankton
107 blooms (Zilius et al., 2013). This shift in primary producers results in a cascade of
108 biogeochemical consequences, including anoxia and organic matter degradation through
109 methanogenesis, that ultimately lead to severely enhanced CH₄ emissions (Bonaglia et al.,
110 2025). Wetland hydrology is one of the key factors regulating ecosystem functioning, as it

111 influences both primary production through water availability and the balance between
112 respiration and methanogenic degradation of organic matter through limitation of oxygen
113 diffusion into the sediments (Cui et al., 2024; Rochera et al., 2025a). However, anoxic
114 conditions do not always result in elevated wetland CH₄ emissions, as the supply of sulfate
115 by saline waters can severely limit methanogenesis through resource competition with
116 more energy-efficient sulfate reduction metabolisms under the right redox conditions
117 (Lovley and Klug, 1983; Miralles-Lorenzo et al., 2025). Emissions of CH₄ are further
118 modulated by the existence of plant-mediated transport mechanisms, which can bypass
119 oxidation back to CO₂ during upward diffusion through oxic sediment horizons (Ge et al.,
120 2024).

121 While the general biogeochemical controls of wetland CO₂ and CH₄ exchanges are relatively
122 well understood, large uncertainty remains on how these interact under practical cases of
123 ecological restoration, leading to poorly constrained climatic mitigation potential (Griscom
124 et al., 2017). Wetland restoration generally enhances CO₂ uptake outweighing increases in
125 CH₄ emissions and resulting in net climate benefits (He et al., 2024). However, existing
126 literature is dominated by studies focused on inland systems (peatlands) and just a few
127 coastal wetland types (mangroves, saltmarshes), which do not capture coastal wetland
128 diversity accurately (Misteli et al., 2025; Taillardat et al., 2020). Other synthesis efforts on
129 coastal wetland restoration focus exceedingly on C sequestration (i.e., *Blue Carbon*),
130 overlooking the large role of CH₄ emissions on the net climatic outcome of wetland
131 restoration (Bertolini and da Mosto, 2021). In addition, while valuable for identifying broad
132 patterns, global syntheses often aggregate the high diversity of wetland types, alteration
133 histories and restoration strategies into a limited number of categories (O'Connor et al.,
134 2020), thereby obscuring relevant contextual factors and limiting process-based effective
135 transferable knowledge for management. Overall, current evidence is still scarce on how
136 coastal wetland restoration influences GHG fluxes (Macreadie et al., 2019; Misteli et al.,
137 2025) and coordinated, multi-site assessments are needed to reveal common controls that
138 are robust across wetland types and restoration pathways.

139 In order to better understand the climate mitigation potential of restoring and conserving
140 European coastal wetlands, this study examines concomitant CO₂ and CH₄ exchanges and
141 their combined carbon dioxide equivalent (CO₂-eq) climatic effect across six diverse
142 European case pilot coastal wetlands: saltmarshes, seagrass meadows, freshwater and
143 brackish marshes, riverine lakes and freshwater coastal lagoons. By explicitly embracing
144 the diversity of coastal wetland types, conservation status, and restoration pathways
145 represented across Europe, we aim to move beyond site-specific assessments and identify
146 common patterns and drivers governing GHG flux responses to alteration and restoration.
147 Using standardized static chamber measurements conducted during four seasonal
148 sampling campaigns, we compare instantaneous GHG exchanges across wetland sites
149 representative of preserved, altered, and restored status. Our objectives are to (i)
150 systematically identify the main biogeochemical drivers controlling CO₂ and CH₄ fluxes in
151 the main European coastal wetland types, and (ii) quantify the extent to which restoration
152 and conservation modify their net climatic effect, expressed as daily CO₂eq fluxes. We
153 hypothesize that (i) the drivers and sensitivity of GHG fluxes to the conservation status differ
154 between CO₂ and CH₄, reflecting their distinct production and consumption pathways, and
155 that (ii) the net climatic response to restoration depends on both the type of anthropogenic
156 alteration and the wetland type considered. At the same time, we expect that consistent

157 cross-system patterns will emerge, allowing the identification of shared controls on GHG
158 fluxes despite the heterogeneity of wetland types and restoration contexts examined.

159 2. Methods

160 2.1. Study areas

161 Six case pilots were strategically selected to cover a wide range of European coastal
162 wetland types, thereby providing a representative sample of the ecosystem and climatic
163 diversity across the continent, covering major European coastlines (Atlantic,
164 Mediterranean, Black Sea, Baltic Sea). The selected case pilots were (**Figure 1**, **Figure S1**):
165 South-West Dutch Delta (DU, intertidal salt marshes, Netherlands), Ria de Aveiro (RI,
166 intertidal seagrass beds, Portugal), Camargue (CA, freshwater marshes and ponds,
167 France), the Valencian wetland Marjal dels Moros (VA, brackish marshes, Spain), Danube
168 Delta (DA, freshwater lakes and ponds with reed beds, Romania) and Curonian Lagoon (CU,
169 freshwater lagoon with reed and submerged vegetation, Lithuania). Within each case pilot,
170 sites representing three conservation statuses were selected in duplicate: preserved,
171 altered, and restored. Preserved sites served as reference systems with unaltered structure
172 and function, whereas altered and restored sites reflected dominant anthropogenic
173 pressures and corresponding restoration measures. Sites within each pilot wetland were
174 geographically close, ensuring comparable climatic conditions and allowing differences in
175 biogeochemical functioning to be attributed to the conservation status. Site characteristics
176 are summarized in **Table 1**, with further details provided in supplementary materials and
177 Oliveira et al. (submitted).



178

179 **Figure 1.** Map showing the location of the six case pilots. Map lines do not necessarily depict accepted national
180 boundaries. Representative pictures can be found in **Figure S1**.

181 **Table 1.** Summary descriptions of studied wetland type, main alterations and restoration
 182 activities for each of the six case pilots.

Case pilot	Wetland type	Alteration	Restoration
South-West Dutch Delta (DU)	Intertidal salt marshes	Erosion-protection coastal infrastructures	Removal of barriers and passive saltmarsh recovery
Ria de Aveiro (RI)	Intertidal <i>Zostera noltii</i> seagrass meadows	Bait-digging, trampling, vegetation loss	Active re-vegetation (transplantation)
Camargue (CA)	Freshwater marshes and ponds	Land-use change and artificial hydrological regime	Habitat reconstruction (Soil, hydrology, morphology, vegetation)
Marjal dels Moros (VA)	Brackish marshes	Desalination, hydromorphological and soil degradation, invasive species	Habitat reconstruction (Soil, hydrology, morphology, vegetation)
Danube Delta (DA)	Freshwater lakes and ponds with reed beds	Land-use change (crops and livestock)	Habitat reconstruction (hydrology, morphology, vegetation)
Curonian Lagoon (CU)	Freshwater littoral with submerged vegetation and reed beds	Water quality (eutrophication)	Passive restoration through the reduction of nutrient load and hydrological changes.

183 2.2. Sampling design

184 A standardized sampling protocol using static chamber GHG flux measurements was
 185 applied across all case pilot wetlands (Minaudo et al., 2023). All 36 sites were sampled once
 186 per season, between October 2023 and August 2024. In each site, the areal proportion of
 187 three land cover strata classes was estimated in advance using aerial photography and
 188 remote sensing images, then confirmed visually upon arrival: (i) open water areas (i.e.,
 189 without emergent vegetation and with >10 cm of water depth), (ii) vegetated areas (i.e.,
 190 covered by emergent vegetation (helophytes, and, for Ria de Aveiro, seagrasses), regardless
 191 of water presence), and (iii) bare areas (i.e., covered by soil or sediment exposed to the
 192 atmosphere at the sampling time). Strata representing <10% of the site area at the time of
 193 the visit were excluded from sampling. Each remaining stratum was sampled with a
 194 minimum of 3 static chamber deployments, with additional deployments allocated
 195 proportionally to stratum areal cover and randomly distributed within each of them. On
 196 each sampling day, an average of 15 ± 2 (mean \pm SD) chamber deployments per site were
 197 performed, depending on logistical constraints.

198 All chamber deployments included a dark incubation to minimize heating effects (Lorke et
 199 al., 2015). In vegetated areas, an additional transparent incubation was performed to
 200 assess the effects of photosynthesis on GHG fluxes. Concentrations of CO₂, CH₄, and H₂O
 201 were measured by recirculating chamber headspace through portable gas analyzers (Li-
 202 COR 7810, Picarro G4301, GLA132-GGA). Incubation start and end times were recorded
 203 manually and, whenever possible, via instrument software. Two different custom-built
 204 static chambers were used depending on the strata. Open water fluxes were measured
 205 using a floating opaque semi-spherical chamber (V = 14.4 L, A = 1134 cm², **Figure S2**) with
 206 10-15 min incubations to capture diffusive and ebullitive fluxes. Bare and vegetated areas
 207 were sampled using a modular transparent cylindrical plexiglass chamber with 3-5 min

208 incubations; collars were inserted 1-3 cm into the sediment and dark conditions were
209 ensured by covering the chamber with an opaque blanket. Chamber volume ($V = 4.6$ to 69
210 L, $A = 460$ cm^2 , **Figure S2**), was adjusted to vegetation height to optimize sensitivity. In
211 flooded vegetated areas, and to avoid mobilization of sediment CH_4 , the chamber was
212 maintained on the water surface either using a flotation ring (**Figure S2**) or holding it by
213 hand. Effective chamber volume was calculated for each deployment based on chamber
214 height above the water and sediment surface.

215 2.3. Flux calculation

216 2.3.1. Instantaneous flux estimates

217 All data treatment, including flux calculations and statistical analyses, was performed in R
218 version 4.5.0 (R Core Team, 2025). Incubation time periods were mapped onto the raw gas
219 concentration time series and start-end times adjusted to exclude instrument and
220 manipulation artefacts after individual visual inspection of each incubation. Ebullitive
221 patterns of CH_4 timeseries were identified but not excluded. A total of 52 CO_2 (1.7%) and 56
222 CH_4 (1.8%) time series were discarded due to severe artifacts or documented manipulation
223 errors. For the remaining 2,990 CO_2 and 2,986 CH_4 time series, instantaneous fluxes were
224 estimated independently for each gas species using three approaches: (i) a two-point
225 method, where the flux was calculated from the net concentration change throughout the
226 incubation using the average (10 s) initial and final concentrations; (ii) a linear model (LM);
227 and (iii) a non-linear (HM) (Hutchinson and Mosier, 1981) regression model. LM and HM
228 models were obtained using the goFlux R package v2.0.0 (Rheault et al., 2024). Areal molar
229 fluxes were calculated for each of the three approaches via the ideal gas law using chamber
230 geometry, and site-specific temperature and atmospheric pressure recorded by the nearest
231 meteorological station. For each gas time series, a best-flux estimate was selected from
232 the three available models following sequential objective criteria (see supplementary
233 materials). The resulting dataset, containing 2,990 CO_2 and 2,986 CH_4 instantaneous fluxes
234 from 2,106 static chamber deployments, is deposited at LifeWatch ERIC (Cabrera-Brufau
235 et al., 2025).

236 2.3.2. Data filtering and pooling of non-vegetated strata

237 To ensure comparability across case pilots and conservation statuses, deployments
238 conducted outside site boundaries or after substantial manipulation (e.g., vegetation
239 removal) were discarded (54 deployments). In the two tidally influenced case pilots (Ria de
240 Aveiro and Dutch delta), deployments during rising and receding tides were also discarded
241 (93 deployments), due to the transient nature of peak-fluxes under these conditions (Lin et
242 al., 2024) and the difficulty of attributing them to the conservation status of the location
243 where they were obtained. Therefore, all subsequent analyses for these case pilots refer
244 only to low-tide conditions. Overall, 147 of the 2,106 deployments with valid fluxes (7%)
245 were excluded from further analysis. Additionally, to ensure strata representativity across
246 statuses and seasons within each case pilot, the three sampled strata were pooled into two
247 classes based on the presence or absence of emergent vegetation (vegetated vs. non-
248 vegetated), enabling robust assessment of strata-specific status effects.

249 2.3.3. Daily temporal integration and calculation of CO_2 equivalent flux

250 Instantaneous fluxes were temporarily integrated into a single net daily flux for each
251 chamber deployment, accounting for stratum-specific incubation availability. For

252 vegetated strata, net daily fluxes were calculated by scaling transparent and dark
253 instantaneous fluxes to the respective daytime and nighttime fractions at each site and
254 date, based on official sunrise and sunset times calculated with the suncalc R package
255 (Thieurmel and Elmarhraoui, 2022). For non-vegetated strata, net daily fluxes were derived
256 either directly from a single dark instantaneous measurement (1,087 chambers, 94.7%) or,
257 when both dark and transparent incubations were available due to visible
258 microphytobenthos (61 chambers, 5.3%), using the same temporal scaling approach
259 applied to vegetated strata. Daily combined climatic effect as CO₂-eq flux was calculated
260 for each chamber deployment using the daily CO₂ and CH₄ fluxes and a 100-year global
261 warming potential factor of 27 for CH₄ mass flux (IPCC, 2023). In total, 1,917 CO₂, 1,916
262 CH₄, and 1,887 CO₂-eq daily fluxes were obtained. Fluxes are reported as daily molar CO₂
263 and CH₄ fluxes per unit area and time, or as daily CO₂-eq mass fluxes per unit area and time
264 (Neubauer, 2021).

265 2.4. Statistical treatment

266 To assess the effects of the conservation status on GHG fluxes, generalized linear mixed
267 effects models (GLMM) were built for each case pilot and net daily flux type (CO₂, CH₄, CO₂-
268 eq). Data was transformed using the bestNormalize package (Peterson, 2021). A pseudo-
269 log transformation from the scales package (Wickham et al., 2025), a variant of a signed-log
270 transformation that transitions to linear scale at low values near zero, was added to the
271 default *bestNormalize* function options, and the transformation that maximized normality
272 was used for each model. Daily flux was modelled as a function of status, season,
273 vegetation presence, and their full interaction as fixed effects. Site was included as random
274 effect to account for repeated samplings across seasons and for site-specific intercepts.
275 Gaussian-distribution models were preferentially used; T-family distribution models were
276 used when gaussian assumptions were not met. For Ria de Aveiro, vegetation presence was
277 not included as fixed effect due to the absence of non-vegetated areas in restored sites.
278 Models were built using the glmmTMB package (McGillycuddy et al., 2025) and validated
279 using DAHRMa diagnostics (Hartig, 2024).

280 Estimated marginal means (EMMs) were derived for relevant fixed effects using the
281 emmeans package (Lenth, 2025). EMMs were weighted by the seasonal areal proportions
282 of vegetated and non-vegetated cover, while maintaining equal seasonal weighting overall;
283 for Ria de Aveiro, equal weights were applied across seasons. Standard errors and
284 confidence intervals accounted for the full variance-covariance structure of each model.

285 To compare fluxes among conservation statuses and estimate restoration and
286 conservation mitigation capacity, post-hoc pairwise contrasts between EMMs were
287 performed using t or z tests (for gaussian or t-family models, respectively) following the
288 emmeans package approach (Lenth, 2025). For each comparison, the difference in EMMs
289 was divided by the standard error of the difference (computed as the square root of the sum
290 of squared standard errors), and two-sided p-values were obtained from the appropriate
291 distribution (normal or t distribution). To account for multiple comparisons within each
292 grouping, p-values were adjusted using the Sidak correction. Letters (Compact Letter
293 Display, CLD) were assigned to significantly different EMMs groups in figures using the
294 multcompView package (Graves et al., 2024). All model-derived estimates (EMMs and
295 contrasts) were back-transformed to original scales. Figures were produced with ggplot2
296 package (Wickham, 2016). A 5% significance threshold was set for all statistical tests.

297 Scripts used for statistical treatment of data and figures can be found in
298 https://github.com/MCabreraBrufau/CabreraBrufau_et_al_2026_code.

299 2.5. Methodological considerations

300 Several limitations affect the representativity of the GHG flux estimates. Static chamber
301 measurements are prone to closing/opening artefacts and non-linear patterns (Maier et al.,
302 2022). These were mitigated through careful handling, timeseries screening, and
303 standardized flux selection, ensuring transparent processing and minimizing subjective
304 biases (Minaudo et al., 2025). Spatially, the highly localized nature of chamber
305 measurements might derive into large variability of wetland-level average fluxes. This was
306 accounted for by the stratified sampling design, ensuring good representation of relevant
307 strata while allowing for the detection of strata-specific effects. Nevertheless, while the
308 employment of modular chambers allowed for coverage of most strata, their dimensions
309 precluded the sampling of large (>1.5 m) vegetation stands, likely resulting in
310 underestimations of CO₂ uptake for reed dominated sites. Temporally, sampling was limited
311 to one low-tide event per season and relied on opaque chambers instead of direct nighttime
312 measurements. Accordingly, the approach was not intended to generate fully scalable site-
313 level GHG budgets, but to enable consistent and unbiased comparisons across
314 conservation statuses to assess the effects of wetland alteration and restoration on GHG
315 exchanges and climate mitigation potential.

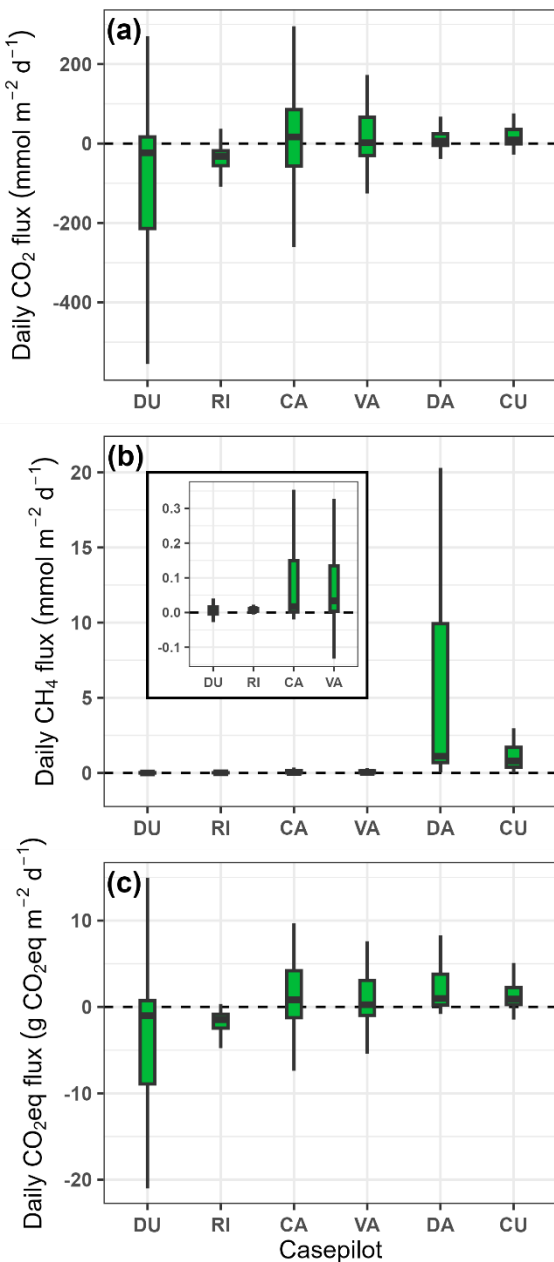
316 3. Results

317 3.1. Fluxes across preserved wetlands

318 Daily net fluxes at preserved sites varied among case pilot wetlands and GHG species
319 (**Figure 2**). Preserved sites generally exhibited daily CO₂ fluxes (mmol CO₂ m⁻² d⁻¹) centred
320 around zero but with substantial variability (**Figure 2a**). Atlantic tidal sites DU (median = -
321 23.2, IQR = -214 to 16.7) and RI (median = -32.4, IQR = -55.7 to -18.2), showed net CO₂
322 uptake, with DU presenting one of the largest flux variabilities. Mediterranean sites
323 exhibited similarly high variability, with CA showing the highest CO₂ flux (median = 16.7, IQR
324 = -56.7 to 85.3) and VA having CO₂ fluxes closest to net zero (median = 2.0, IQR = -30.2 to
325 66.1). Eastern sites showed similar CO₂ flux profiles, with intermediate median fluxes and
326 relatively low variability for DA (median = 6.07, IQR = -4.82 to 24.4) and slightly higher fluxes
327 for CU (median = 9.1, IQR = -0.8 to 35.4).

328 Net daily CH₄ fluxes (mmol CH₄ m⁻² d⁻¹) were generally positive across all preserved sites,
329 with higher median emissions associated with greater variability and strongly skewed
330 distributions (**Figure 2b**). Atlantic tidal wetlands showed the lowest CH₄ emissions, with
331 similar values at DU (median = 1.5×10^{-3} , IQR = -4.2×10^{-3} to 1.6×10^{-2}) and RI (median = 8.3×10^{-3} , IQR = 4.4×10^{-3} to 1.2×10^{-2}). Mediterranean preserved sites exhibited intermediate
332 CH₄ emissions, with CA (median = 1.7×10^{-2} , IQR = 1.8×10^{-3} to 1.5×10^{-1}) showing lower
333 median fluxes than VA (median = 3.4×10^{-2} , IQR = 3.4×10^{-2} to 1.4×10^{-1}) but comparable
334 variability. Eastern preserved sites showed the highest emissions, with DA (median = 1.1,
335 IQR = 0.7 to 9.9) displaying the highest CH₄ fluxes and extreme skewness, while CU (median
336 = 0.8, IQR = 0.4 to 1.7) had lower and less variable CH₄ fluxes.

338 The contrasting CO₂ and CH₄ flux profiles at preserved sites resulted in CO₂-eq distributions
 339 reflecting the dominant contributor to climatic forcing in each case pilot (**Figure 2c**). CO₂
 340 generally dominated the CO₂-eq balance, with CH₄ contributing minor proportions (mean \pm
 341 SD) in Atlantic (2 \pm 5% in both DU and RI) and Mediterranean (8 \pm 19 in CA, 7 \pm 17 in VA)
 342 sites, but substantially higher shares in eastern wetlands (50 \pm 32% in DA, 35 \pm 27% in CU).
 343 Regarding CO₂-eq fluxes (g CO₂ eq. m⁻² d⁻¹), values were lowest in the Atlantic tidal wetlands
 344 RI (median = -1.5, IQR = -2.5 to -0.9) and DU (median = -1.0, IQR = -8.9 to 0.7), intermediate
 345 in the Mediterranean wetlands VA (median = 0.3, IQR = -1 to 3.1) and CA (median = 0.8, IQR
 346 = -1.3 to 4.2) with ranges spanning net zero, and highest in the eastern wetlands CU (median
 347 = 0.9, IQR = 0.3 to 2.3) and DA (median = 1, IQR = 0.2 to 3.8) with ranges above net zero.

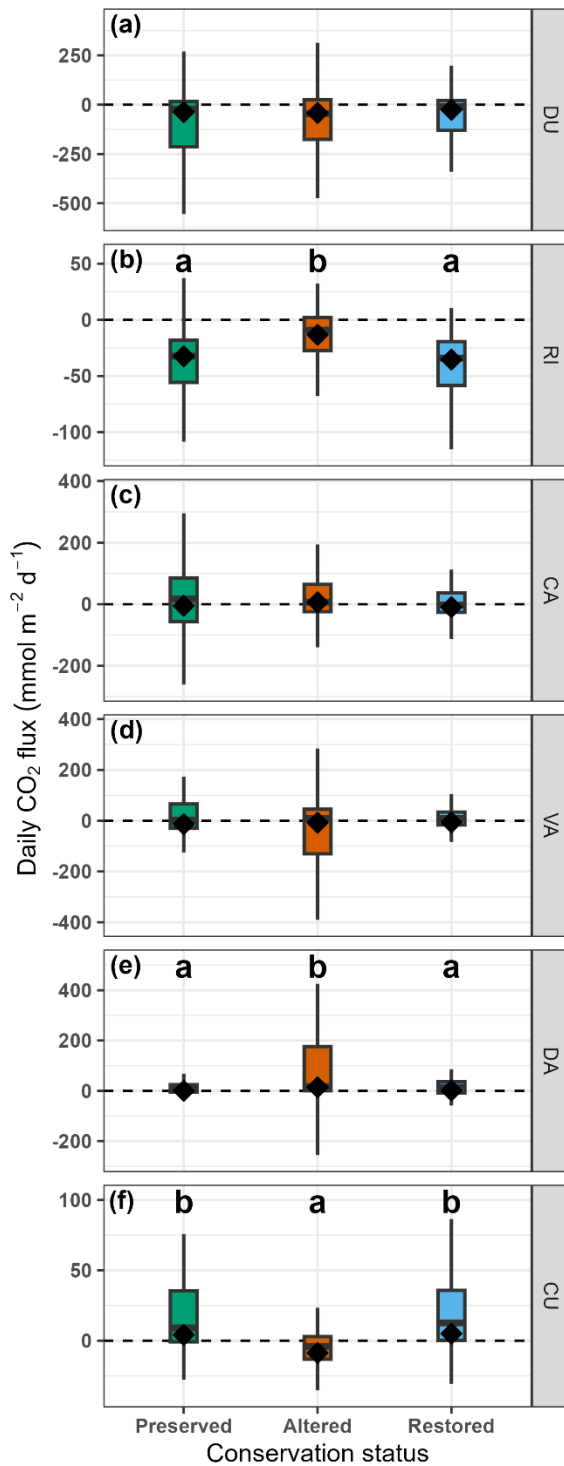


348

349 **Figure 2.** Daily fluxes across preserved case pilot wetlands of (a) CO₂, (b) CH₄, and (c) combined CO₂-eq. Boxplots show the
 350 median, interquartile range (IQR), and whiskers extending to 1.5xIQR; potential outliers (data outside the previously defined
 351 ranges) are not displayed for clarity. Inset in (b) shows a zoomed-in view of CH₄ flux data for DU, RI, CA, and VA to better
 352 visualize differences; y-axis scale differs from the main panel.

353 3.2. Effect of conservation status on CO₂ fluxes

354 Daily CO₂ fluxes (mmol m⁻² d⁻¹) showed wetland-specific patterns related to the
355 conservation status (**Figure 3**). Significant status effects were detected in three case pilot
356 wetlands (RI, DA, CU) (**Table S1**), with clear differences between preserved, altered, and
357 restored sites (**Table S3**). In RI and DA, altered sites exhibited significantly higher CO₂ fluxes
358 than preserved ($p \leq 0.004$) and restored ($p < 0.001$) sites, which showed similar low fluxes
359 ($p \geq 0.81$). In contrast, CU displayed lower CO₂ fluxes in altered sites compared to preserved
360 ($p < 0.001$) and restored ($p < 0.001$) sites. No statistically significant status effects were
361 observed in DU, CA, or VA, where CO₂ fluxes were comparable across conservation
362 statuses. Beyond status, CO₂ fluxes were consistently influenced by seasonality and
363 vegetation presence, often interacting with the conservation status, even when status alone
364 was not significant (**Table S1, Figures S3 and S6**).



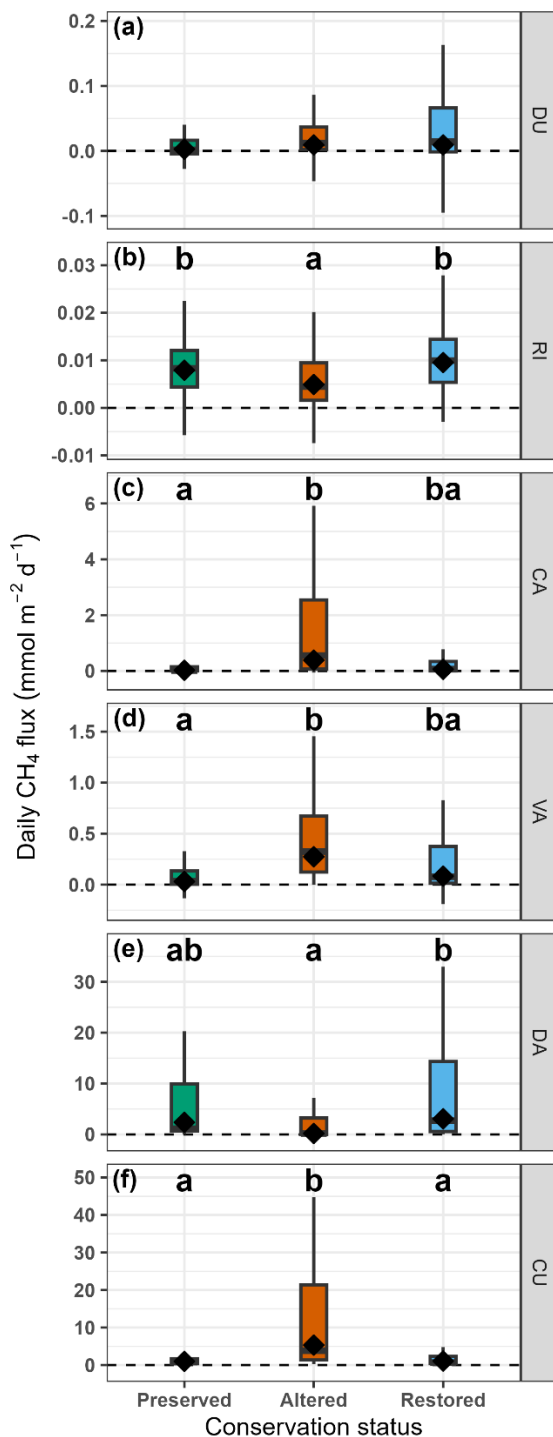
365

366 **Figure 3.** Daily CO₂ fluxes (mmol m⁻² d⁻¹) according to conservation status for each case pilot wetland. Boxplots show the
 367 median, interquartile range (IQR), and whiskers extending to 1.5xIQR; potential outliers (data outside the previously defined
 368 ranges) are not displayed for clarity. Diamonds represent GLMM-derived EMMs and letters are shown in panels with
 369 significantly distinct EMMs groups ($p<0.05$, post-hoc t.test or z.test, **Table S3**) alphabetically ordered according to group ranks.

370 **3.3. Effect of conservation status on CH₄ fluxes**

371 CH₄ fluxes (mmol m⁻² d⁻¹) showed clearer and more consistent responses to conservation
 372 status across case pilot wetlands (**Figure 4**). Significant status effects were detected in all
 373 case pilot wetlands except DU (**Table S1**), where CH₄ fluxes did not differ among preserved,

374 altered and restored sites (**Table S3**). In RI, preserved and restored sites exhibited slightly
 375 higher CH₄ fluxes than altered sites ($p = 0.004$, and $p < 0.001$, respectively). In the
 376 Mediterranean wetlands (CA and VA), altered sites showed higher CH₄ emissions than
 377 preserved sites ($p \leq 0.041$), with restored sites displaying intermediate fluxes. In DA,
 378 restored sites had higher CH₄ fluxes than altered sites ($p = 0.044$), while preserved sites
 379 were intermediate. In CU, altered sites exhibited substantially higher CH₄ emissions than
 380 both preserved ($p = 0.002$) and restored ($p = 0.004$) sites, which showed similarly low fluxes.
 381 As for CO₂, CH₄ flux variability was strongly influenced by seasonality across all case pilots
 382 and by vegetation presence in most cases, with frequent interactions between the
 383 conservation status, season, and vegetation presence (**Table S1**; **Figure S4 and S7**).

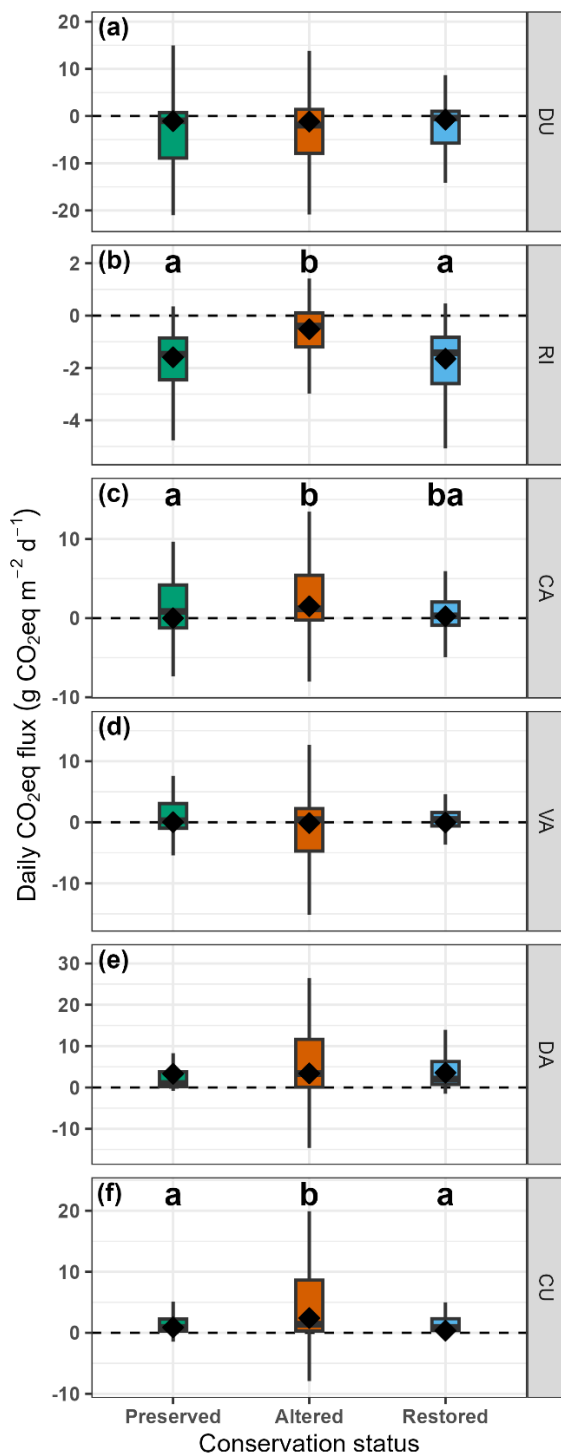


384

385 **Figure 4.** Daily CH₄ fluxes (mmol m⁻² d⁻¹) according to conservation status for each case pilot. Boxplots show the median,
386 interquartile range (IQR), and whiskers extending to 1.5xIQR; potential outliers (data outside the previously defined ranges)
387 are not displayed for clarity. Diamonds represent GLMM-derived EMMs and letters are shown in panels with significantly
388 distinct EMMs groups ($p < 0.05$, post-hoc t.test or z.test, **Table S3**) alphabetically ordered according to group ranks.

389 3.4. Effect of conservation status on CO₂-eq fluxes

390 The effects of the conservation status on combined CO₂-eq fluxes (**Figure 5**) were less
391 consistent than for CO₂ and CH₄ alone. Significant status effects were detected in RI, CA,
392 DA and CU (**Table S1**), with significant differences among altered, preserved and restored
393 locations in RI, CA and CU (**Table S3**). No statistically significant status effect was observed
394 in DU and VA ($p \geq 0.76$), where CO₂-eq fluxes were similar across preserved, altered, and
395 restored sites. In RI and CU, preserved and restored sites showed comparable CO₂-eq
396 fluxes ($p \geq 0.34$) that were lower than those of altered sites ($p \leq 0.046$). In CA, preserved sites
397 had lower CO₂-eq fluxes than altered sites ($p = 0.018$), with restored sites showing
398 intermediate values. Although DA showed a significant overall status effect, differences
399 among estimated marginal means were not significant. Across case pilots, seasonality and
400 vegetation presence strongly influenced CO₂-eq fluxes and frequently interacted with the
401 conservation status where status effects were present (**Table S1**, **Figure S5**, **Figure S8**).



402

403 **Figure 5.** Daily CO₂-eq flux (g CO₂ eq. m⁻² d⁻¹) according to conservation status for each case pilot wetland. Boxplots show the
 404 median, interquartile range (IQR), and whiskers extending to 1.5xIQR; potential outliers (data outside the previously defined
 405 ranges) are not displayed for clarity. Diamonds represent GLMM-derived EMMs and letters are shown in panels with
 406 significantly distinct EMMs groups ($p<0,05$, post-hoc t.test or z.test, **Table S3**) alphabetically ordered according to group ranks.

407 **4. Discussion**

408 **4.1. Biogeochemical drivers of gaseous C exchange in European coastal**
409 **wetlands**

410 Across the wetlands examined, the effects of conservation status on CO₂, CH₄ fluxes varied
411 among the studied wetland types, main types of alterations and associated restoration
412 measures. CO₂ fluxes showed variations associated with the conservation status in only
413 three of six case pilots, whereas CH₄ fluxes were more responsive, with significant effects
414 in five of six case pilots. Wherever status effects were detected for CO₂, they were
415 consistently opposite in direction to those of CH₄, reflecting contrasting conditions that
416 control the underlying processes regulating CO₂ and CH₄ exchanges in the different
417 wetlands considered, with enhancement of aerobic conditions increasing CO₂ release,
418 while actions favoring anaerobic conditions (e.g., rewetting) increased CH₄ emissions.
419 Despite this variability, mostly depending on the specific features of each wetland type and
420 the conservation status of sites, some common mechanisms were evident across wetland
421 types.

422 The diversity of wetland types and ecological conditions examined allowed identification of
423 key drivers of CO₂ and CH₄ exchanges, strongly modulated by seasonality. CO₂ fluxes were
424 primarily controlled by vegetation cover and sediment oxygen availability, which regulated
425 the balance between photosynthetic uptake and respiration-mediated release of CO₂.
426 Emissions of CH₄ were mostly related to hydrology-driven oxygen availability in the
427 sediment, salinity conditions, and presence of reed-type vegetation, with labile organic
428 matter supply being important in some systems. CO₂ exchange responded mostly to
429 alteration and restoration actions that severely modified the landscape of the wetlands,
430 either through substantial loss or gain in abundance of primary producers or through
431 profound changes in inundation patterns related to land-use change. CH₄ emissions were
432 more sensitive to subtler hydrological changes, either through variations in water quality
433 and salinity or through hydrodynamics modifying the extent and timing of wetlands flooding
434 and water table depths. This sensitivity is strongly seasonal and temperature-driven, an
435 effect that becomes increasingly evident at lower latitudes. Global changes that extend
436 warm periods could potentially extend the duration of the observed seasonal CH₄ emission
437 peaks in summer(Camacho et al., 2017; Morant et al., 2024); thus, accounting for seasonal
438 variability is essential to accurately assess restoration outcomes, or the consequences of
439 their absence.

440 Emergent vegetation presence exerted strong and consistent impact on CO₂ fluxes across
441 all wetland types where it was evaluated, with vegetated areas generally acting as net CO₂
442 sinks (**Table S1; Figure S6**). This evidences that, although strongly regulated by seasonality
443 and local climatic conditions, vegetation standing stock is a primary driver of ecosystem-
444 level primary production through photosynthetic uptake of CO₂ (Reddy et al., 2022). While
445 our statistical framework could not explicitly include this effect for the seagrass meadows
446 of Ria de Aveiro, the expected stronger CO₂ uptake by *Zostera noltii* meadows with respect
447 to bare mudflats becomes evident when considering the strong differences in vegetated
448 coverage between the sites of different conservation status sampled. RI altered sites
449 suffered from erosion, bait-digging and trampling (**Table 1**), which reduced their *Z. noltii*
450 coverage to an average of 8%. Instead, preserved sites as well as restored sites after

451 seagrass planting showed much higher average *Z. noltii* coverages (61% and 96%,
452 respectively), which is the likely explanation behind the significantly enhanced CO₂ uptake
453 shown by these sites (**Figure 3b**).

454 Plant community composition is also sometimes shown to influence overall CO₂ uptake
455 rates in wetlands (Ward et al., 2009). Several of the wetlands studied suffered from
456 alterations that involved modified vegetation communities such as presence of invasive
457 species and loss of native vegetation and land use change (**Table 1**). Generally, the CO₂
458 exchange profile in vegetated areas of different conservation status did not reveal
459 significant differences (**Figure S6**), indicating that environmental alterations related to
460 shifts in plant community composition had little impact on CO₂ exchange in the studied
461 wetlands. While vegetation composition is a good indicator of the overall ecological
462 integrity of wetland systems, the potential biogeochemical effects of these types of shifts
463 (Davidson et al., 2018) were not of sufficient magnitude to be detected in our study.
464 Although the vegetated areas of the Danube Delta wetlands did show significant differences
465 that might be associated with differences in primary productivity of reed stands and
466 agricultural crop species (**Figure S6**), these coincided with permanently inundated
467 substrates and agricultural soils, respectively. Thus, the observed differences likely arise
468 from two main factors: differences in vegetation primary production efficiency and lower
469 aerobic respiration rates due to oxygen limitation in submerged sediments and the water
470 column compared with well-aerated agricultural soils (Bianchi et al., 2021). This
471 interpretation is supported by the higher CO₂ emissions measured in non-vegetated areas
472 of altered sites relative to preserved and restored sites in the Danube Delta (**Figure S6**).
473 These two non-exclusive mechanisms likely resulted in the status-level differences in CO₂
474 fluxes observed in the Danube Delta (**Figure 3e**). Finally, the abundance of other primary
475 producers (phytoplankton) appears to be the dominant driver responsible for the CO₂
476 exchange profiles observed in the Curonian Lagoon (**Figure 3f**). In this wetland, nutrient
477 load was the main alteration factor related to conservation status and ecosystem
478 interventions (**Table 1**), leading to eutrophication and associated massive phytoplankton
479 blooms in altered sites (Vaičiūtė et al., 2021; Zilius et al., 2013), as indicated by water
480 chlorophyll-a concentrations (**Table S4**). Thus, enhanced CO₂ uptake and reduced
481 respiration under anoxic conditions driven by organic C accumulation by phytoplankton in
482 open water areas (**Figure S6**) seem to be the main drivers behind the general status-level
483 differences in CO₂ exchange profiles of the Curonian Lagoon (**Figure 3f**).

484 Hydrology emerged as a dominant control on CH₄ exchanges across the wetlands studied.
485 Permanently flooded sediments promote anoxic conditions that favor methanogenesis
486 (Camacho-Santamans et al., 2025; Rochera et al., 2025b) while restricting aerobic
487 respiration and thus CO₂ releases. This mechanism is exemplified by the general inter-
488 wetland type variability observed for CH₄ (**Figure 2**), where freshwater systems
489 characterized by permanently flooded conditions, where salinity does not control
490 methanogenesis (Camacho et al., 2017; Miralles-Lorenzo et al., 2025; Morant et al., 2024),
491 such as Danube Delta lakes and the Curonian Lagoon, present by far the largest emission
492 profiles of CH₄. A similar pattern was observed for the freshwater marshes of Camargue,
493 where wetland hydrology was a main determinant of the conservation status (**Table 1**) and
494 CH₄ emissions (**Figure 4c**). CA altered sites hydrodynamics favored flooded conditions, as
495 reflected by 73 % of chamber deployments in these sites occurring in inundated areas with
496 respect to 48% for preserved sites. Accordingly, altered sites presented overall higher CH₄
497 emissions (**Figure 4c, Table S3**), particularly during the summer season (**Figure S4**),

498 coinciding with highest discrepancy in flooded area proportion between altered and
499 preserved sites (82% vs. 40%) and high temperatures that likely limited oxygen availability
500 and enhanced microbial activity in submerged sediments (Cui et al., 2024). Modified
501 hydrology was also an important factor regulating CH₄ emissions in the brackish
502 Mediterranean marshes of Marjal dels Moros, where similar patterns in inundation
503 proportion (65% vs 26%) were likely contributing to the higher CH₄ emissions observed in
504 altered sites, with respect to preserved ones (**Figure 4d**).

505 Nevertheless, CH₄ emissions were not only influenced by hydrology-driven oxygen
506 availability of the sediments but also by another of the main regulating factors of CH₄
507 production in coastal wetlands, namely salinity. Through the provision of sulfate as a more
508 energetically favorable electron acceptor than CO₂, seawater intrusion regulates the
509 dominance of sulfate-reducing over methanogenic microbes (Koepsch et al., 2019;
510 (Miralles-Lorenzo et al., 2025). This mechanism helps to explain the gradient in CH₄
511 emissions observed along the progressively more saline altered, restored and preserved
512 sites of Marjal dels Moros (**Figure 4d, Table S4**). Additionally, this salinity-driven
513 methanogenesis limitation in tidal wetlands such as DU saltmarshes and RI *Z. noltii*
514 meadows is likely responsible for their extremely low CH₄ emissions with respect to the
515 other coastal wetlands examined (**Figure 2**).

516 While anoxia and salinity help to regulate the dominant catabolic metabolism in sediments,
517 the supply of different organic matter substrates is one of the principal factors regulating
518 the overall rates of organic C degradation, and CH₄ emissions (Rissanen et al., 2023). Across
519 the wetlands examined, the effect of labile organic matter supply in regulating CH₄
520 production can help to explain small but significantly higher CH₄ emissions of preserved
521 and restored *Z. noltii* meadows with respect to bare altered sites of RI (**Figure 4b**), as
522 seagrasses produce and release methylated compounds that represent an attractive
523 substrate for methanogens (Schorn et al., 2022). Of more relevance is the pattern observed
524 in the Curonian Lagoon wetland, where enhanced phytoplankton growth fueled by
525 increased nutrient loads (**Table S4**) resulted in an accumulation of labile organic matter in
526 the sediments of altered sites (Remeikaite-Nikiene et al., 2016). Rapid degradation of
527 phytoplankton-derived organic-C leads to anoxic conditions which, together with the
528 freshwater character of the sites (Zilius et al., 2013), resulted in an ideal environment for
529 methanogenesis, helping to explain the stark differences in CH₄ overall emissions between
530 the altered and preserved and restored sites of this wetland (**Figure 4f**). Additionally,
531 although these increased emissions of CU eutrophic sites were consistently detected in
532 both open-water and vegetated areas, the magnitude of CH₄ emissions was much higher in
533 reed-covered zones of CU, which is a common pattern observed across many of the
534 wetlands examined (**Figure S7**). The consistently higher CH₄ emissions observed in
535 vegetated zones likely result from vegetation-facilitated transfer of CH₄ from sediments to
536 the atmosphere, bypassing oxidation in sediments and the water column (Ge et al., 2024).
537 However, this enhanced CH₄ release generally does not exceed photosynthetic C
538 assimilation when assessed in terms of net C balance.

539 Across wetlands, two non-exclusive mechanisms emerged as primary drivers of changes in
540 GHG exchange: shifts in areal habitat composition and changes in process rates within
541 habitats. Major alterations and restoration actions can modify wetland structure to the
542 point where entire habitats are lost along with their biogeochemical functioning. The loss
543 and replantation of seagrass beds in Ria de Aveiro or the land-use changes of the Danube

544 Delta wetlands are extreme examples of this mechanism. Conversely, subtler interventions
545 that do not visually alter the ecosystem landscape can nonetheless shift underlying
546 processes and result in significant impacts on biogeochemical process rates. The
547 degradation and subsequent recovery of water quality in the Curonian Lagoon through
548 regulation of nutrient-loads is a good example for this process: while the composition of
549 open water and reed beds habitats remained the same between altered and restored sites,
550 their habitat-specific rates of CO₂ and CH₄ production and atmospheric exchange were
551 significantly different (**Figures S6, S7**). While the above examples represent extremes of
552 these two mechanisms, it is important to recognize the existence of a continuum between
553 them. It is also important to acknowledge that no single habitat-specific “reference” rate
554 exists for any natural process. In this context, seasonal variability regulates GHG fluxes
555 through two pathways: temperature and physiological shifts alter habitat-specific process
556 rates, while seasonal flooding dynamically redistributes the relative extent of open water,
557 vegetated areas, and bare sediments within wetlands.

558 The contrasting sensitivities and drivers of CO₂ and CH₄ often led to opposite flux responses
559 to the same environmental interventions, making CO₂-eq outcomes dependent on wetland-
560 specific gas dominance. Three general response groups emerged. In tidal wetlands (Dutch
561 Delta and Ria de Aveiro), constant seawater supply suppressed CH₄ emissions to the point
562 that this gas only represented an average 3% and 2% of CO₂-eq exchanges, respectively. In
563 these wetlands, only vegetation-related interventions resulted in a significant impact on
564 their climatic functionality, with changes in CO₂ fluxes outbalancing all detected variations
565 in CH₄ emissions. In seasonally inundated Mediterranean marshes (Camargue and Marjal
566 dels Moros), CH₄ played a moderate role in their CO₂-eq fluxes (18% and 11%, respectively).
567 In these wetlands, CO₂-eq flux changes were detected only when interventions strongly
568 affected CH₄ emissions. In permanently flooded freshwater wetlands (Danube lakes and
569 Curonian Lagoon), CH₄ represented a higher average proportion of the wetland GHG
570 balance in terms of CO₂-eq (43% and 46%, respectively). In these wetlands, ecosystem
571 interventions had clear but opposite effects for CO₂ and CH₄ exchanges, which only
572 resulted in changes of combined CO₂-eq fluxes when CO₂ responses were of relatively low
573 magnitude and outbalanced by strong CH₄ changes.

574 4.2. Climate change mitigation potential of coastal European wetland 575 restoration and conservation

576 This study offers valuable insights into the potential of European coastal wetland
577 restoration as a climate mitigation tool through the exemplary results obtained from six
578 diverse pilot wetlands. Comparison of CO₂, CH₄ and CO₂-eq exchange balances between
579 altered and restored sites provide a quantitative estimate of the mitigation capacity of
580 restoration across different wetland types (**Table S3**).

581 Although the central distributions of daily net fluxes showed apparent reductions in GHG
582 fluxes following restoration in several pilot wetlands (**Figures 3, 4, 5**), driven by significant
583 effects of the conservation status (**Table S1**), high data variability precluded the detection
584 of statistically significant mean flux reductions in some cases (**Table S3**). Across the pilot
585 wetlands, statistically significant mitigation capacity of CO₂ fluxes was only detected for the
586 restoration of Ria de Aveiro seagrass meadows and Danube Delta freshwater lakes, likely
587 driven by increased net primary production of seagrass with respect to bare sediment areas
588 and reduced organic C decomposition rates in freshwater lakes compared with agricultural

589 land use, respectively. For CH₄ fluxes, statistically significant mitigation was only observed
590 following water quality improvement of the Curonian Lagoon, while restoration of natural
591 hydrodynamics in Camargue achieved marginal CH₄ reductions that approached statistical
592 significance. When CO₂ and CH₄ were combined as CO₂-eq, statistically significant
593 mitigation potential was statistically significant only for seagrass replantation in Ria de
594 Aveiro and re-oligotrophication in the Curonian Lagoon.

595 The results show mitigation potential for restoration of some types of degraded coastal
596 European wetlands; however, the cumulative nature of GHG emissions must be
597 considered. Even in cases where restoration completely reverts the biogeochemical
598 functioning of a degraded wetland back to pristine conditions, the net effect must account
599 for the time during which the wetland presented increased emissions incurring in a
600 “recovery debt” (Moreno-Mateos et al., 2017). While the limited potential impact of
601 restoration might appear discouraging, the same temporal consideration highlights the
602 elevated and persistent costs of inaction and the necessity to avoid degradation of coastal
603 wetlands in the first place. In fact, considering the differences in GHG profile associated to
604 sites of preserved and degraded conservation status reveals clear trends that demonstrate
605 the high mitigation potential of maintaining coastal European wetlands in good
606 conservation status (**Table S3**). Potentially avoided emissions through conservation were
607 generally of similar or higher magnitude than those associated with restoration and
608 achieved statistical significance in more cases. These patterns reveal fundamental
609 differences in the functioning of well preserved and restored ecosystems.

610 Restoration projects guided by ecological restoration theory typically focus on alleviating
611 pressures through passive restoration and reconstructing ecosystem structures to
612 accelerate inherent functional recovery via active restoration (Palmer et al. 2016). However,
613 even when restoration is well implemented, functional recovery often lags structural
614 recovery due to slow reestablishment of natural biotic networks underpinning
615 biogeochemical processes (Moreno-Mateos et al., 2012). Additionally, hysteretic dynamics
616 in the face of ecosystem degradation and recovery may lead to trajectories favouring
617 unintended alternative degraded states (Suding et al., 2004). Overall, the risks inherent to
618 wetland restoration, recovery pathways and generally slow biogeochemical functional
619 recovery emphasizes the importance of preserving natural wetlands in a good conservation
620 status.

621 Despite the differences shown above, conservation and restoration are complementary
622 tools for climate mitigation and should not be viewed as alternative management strategies.
623 It is important to recognise that our current assessment of restoration’s mitigation capacity
624 does not account for other biogeochemically relevant benefits, such as expansion of
625 wetland extent or reductions of nitrous oxide (N₂O) emissions (Kasak et al., 2021; Leo et al.,
626 2019), and represents only a snapshot of the functional recovery process likely to improve
627 over time (Moreno-Mateos et al., 2017). Thus, the lack of statistically significant reductions
628 in areal CO₂ and CH₄ exchanges reported in **Table S3** should not be interpreted as evidence
629 that wetland restoration lacks climate mitigation benefits. Moreover, none of the restoration
630 strategies implemented across the different wetlands examined targeted GHG mitigation
631 as an explicit primary objective (Oliveira et al., under review). Therefore, the detected
632 effects on GHG exchanges can be considered as an additional co-benefit to the impact of
633 restoration in improving other ecosystem services such as biodiversity, water quality and
634 flood risk mitigation (Meli et al., 2014; Singh et al., 2019; Wu et al., 2023). Ultimately,

635 although the results show that restoration caused significant increases in emissions of
636 either CO₂ or CH₄ in some wetlands, these were always accompanied by similar or greater
637 changes in the opposite direction for the other GHG species studied. Therefore, when
638 considering the overall climatic impacts attributable to restoration, the only significant
639 effects detected for CO₂-eq exchanges were net reductions, indicating the generation of a
640 climatic cooling capacity (**Table S3**).

641 This study highlights the diverse biogeochemical controls on GHG regulation across
642 European coastal wetlands under different conservation statuses. These functional and
643 site-specific differences must be explicitly considered in restoration and management
644 planning to avoid trade-offs with other ecosystem services (Pörtner et al., 2021).
645 Restoration strategies should therefore incorporate targeted, long-term monitoring to track
646 wetland recovery and detect structural or functional deviations that require corrective
647 action.

648 Wetlands have been heavily impacted by land-use change due to the historical
649 undervaluation of their ecosystem services, often favouring higher-value uses despite
650 substantial ecological losses (Zorrilla-Miras et al., 2014). This underscores the need to
651 explore financing mechanisms that recognize the economic value of wetland ecosystem
652 services, particularly their potential for climate mitigation. However, wetland climate
653 mitigation capacity arises from complex, system-specific interactions among multiple
654 GHGs, characterized by high spatial and temporal variability. Financing schemes should
655 therefore be linked to comprehensive, long-term monitoring of all relevant GHG fluxes to
656 avoid incomplete accounting and over-crediting risks prevalent in current carbon offset
657 markets (Romm et al., 2025). Ultimately, for coastal wetland restoration be an effective
658 nature-based climate solution, projects must demonstrate additionality, feasibility, and
659 permanence, and provide enough evidence to accurately quantify their climate benefits
660 (Jones et al., 2024).

661 Currently, estimates of climate mitigation capacity of wetland restoration are highly variable
662 (Griscom et al., 2017), stemming from incomplete understanding of several climate relevant
663 processes. A common identified issue is the lack of widespread data on how GHG
664 exchanges, in particular CH₄ and N₂O emissions, respond to coastal wetland restoration
665 (Rosentreter et al., 2021). While the climatic effect of restoration projects in other
666 ecosystems might be well represented by simple C balance assessments, in wetlands
667 systems monitoring of these non-CO₂ GHG exchanges is essential to accurately quantify
668 net climatic impact (Macreadie et al., 2019). Transient increases in CH₄ emissions from
669 restored wetlands can, considering radiative forcings and atmospheric lifetimes of GHGs,
670 considerably delay climatic benefits of increased C storage (Schuster et al., 2024).
671 Therefore, wetland restoration actions that achieve timely reductions of CH₄ emissions,
672 such as those of Curonian Lagoon and to a lesser extent Camargue and Marjal dels Moros,
673 become especially relevant to meet climatic mitigation targets. Additionally, the
674 importance of lateral C and off-site GHG exchanges is increasingly being recognized, and
675 future studies should therefore aim to obtain a more complete assessment of watershed-
676 level budgets that support management decisions (Jones et al., 2024; Regnier et al., 2022).
677 Finally, appropriate pre-restoration baseline reference conditions measurements are
678 essential to provide actionable knowledge to managers, thereby allowing quantification of
679 actual benefits of alteration-specific reversals.

680 Given the ample and clear benefits of coastal wetland restoration on the provisioning of
681 other ecosystem services, widespread restoration of degraded systems should
682 nonetheless be pursued. We advocate to taking advantage of recent policy momentum,
683 exemplified by the EU Nature Restoration Regulation, to gather more evidence on the
684 effects of coastal wetland restoration on GHG regulation, enabling us to quantify more
685 precisely the magnitude, consistency and reliability of associated climatic benefits.

686 **5. Conclusions**

687 This study examined how the conservation status and restoration of diverse European
688 coastal wetlands influence atmospheric exchanges of CO₂ and CH₄ and their combined
689 effects on climate forcing expressed as CO₂eq. The results of this study show that GHG
690 fluxes respond differently to degradation and restoration actions depending on the wetland
691 type and associated main biogeochemical drivers. In particular, CO₂ fluxes responded
692 primarily to landscape-scale changes in vegetation cover and inundation, whereas CH₄
693 exchanges were more sensitive to environmental modification and readily responded to
694 comparatively subtle changes in water quality, salinity, and hydrodynamics.

695 These contrasting responses, joined with different relative contributions of CO₂ and CH₄ to
696 net climatic forcing, translated into wetland-specific CO₂eq mitigation potentials
697 associated with restoration and conservation. Replantation of seagrass meadows and
698 eutrophication reversal through improved water treatment emerged as effective restoration
699 measures for increasing climate mitigation capacity of degraded wetlands. Other actions,
700 such as the reestablishment of natural salinity and hydrodynamics regimes showed signs
701 of reducing CH₄ emissions, but high CO₂ flux variability precluded detection of significant
702 reductions in combined CO₂-eq emissions with the measured data.

703 While this study did not assess potential changes in N₂O emissions, the observed patterns
704 for CO₂ and CH₄ contribute to the growing body of evidence supporting wetland restoration
705 as an effective nature-based solution for climate change mitigation. At the same time, the
706 findings of our study underscore the importance of considering multiple GHG and their
707 specific biogeochemistry when evaluating the climatic impact of wetland restoration
708 projects. Further research should therefore aim to simultaneously quantify exchanges of
709 CO₂, CH₄ and N₂O over management-relevant timeframes to better characterize the
710 functional recovery process and obtain more complete assessments of the climatic
711 benefits associated to wetland restoration.

712 Within the scope of this study, restoration projects implemented across a range of
713 European coastal wetland types showed no evidence of significant detrimental effects in
714 terms of CO₂eq. Instead, the results demonstrate that restoration can enhance or, at
715 minimum, maintain climate regulation functions. Joined with ample evidence for other
716 ecosystem service co-benefits, the results of our study support current regulatory efforts
717 aimed at recovering historically degraded European wetlands while underscoring the need
718 for targeted, ecosystem-specific restoration strategies to maximize climate mitigation
719 potential.

720

721 Acknowledgments

722 Funding for this research came from the project
723 RESTORE4Cs - *Modelling RESTORation of wetlands for Carbon pathways, Climate Change*
724 *mitigation and adaptation, ecosystem services, and biodiversity, Co-benefits* (DOI:
725 10.3030/101056782), funded by the European Union under the Horizon Europe research
726 and innovation programme (Grant Agreement ID: 101056782). The views and opinions
727 expressed are those of the author(s) only and do not necessarily reflect those of the
728 European Union or the granting authority. Neither the European Union nor the granting
729 authority can be held responsible for them. We also acknowledge the support of FCT
730 – Fundação para a Ciência e a Tecnologia I.P., to CESAM-Centro de Estudos do Ambiente e
731 do Mar, under the project references UID/50017/2025
732 (doi.org/10.54499/UID/50017/2025) and LA/P/0094/2020
733 (doi.org/10.54499/LA/P/0094/2020). We thank Ana Ribeiro for logistical support. Work by
734 the University of Valencia was also co-supported by projects CLIMAWET-CONS (PID2019-
735 104742RB-I00), funded by the Agencia Estatal de Investigación of the Spanish Government,
736 and by the project ECCAEL (PROMETEO CIPROM-2023-031), funded by the Generalitat
737 Valenciana, both granted to Antonio Camacho.

738 **Declaration of generative AI and AI-assisted technologies in the manuscript 739 preparation process**

740 During the preparation of this work the authors used ChatGPT-5.2 in order to identify
741 potential improvements in text readability and for coding syntax support during data
742 processing. After using this tool/service, the authors reviewed and edited the content as
743 needed and take full responsibility for the content of the published article.

744 **Data and code availability**

745 Data presented in this article is deposited at LifeWatch ERIC
746 (<https://doi.org/10.48372/C29B-QW38>) and will be fully accessible after December 31st,
747 2027. During embargo period, data will be made available upon reasonable request. Code
748 to reproduce results of this article is fully accessible at:
749 https://github.com/MCabreraBrufau/CabreraBrufau_et_al_2026_code.

750 **References**

751 Airoldi, L., Beck, M., 2007. Loss, status and trends for coastal marine habitats of Europe, in: Gibson, R.N., Atkinson, R.J.A., Gordon, J.D.M. (Eds.), *Oceanography and Marine Biology: An Annual Review*. CRC Press, pp. 1–566.
752 <https://doi.org/10.1201/9781420050943>

753

754

755 Bertolini, C., da Mosto, J., 2021. Restoring for the climate: a review of coastal wetland
756 restoration research in the last 30 years. *Restor Ecol* 29, e13438.
757 <https://doi.org/10.1111/rec.13438>

758 Bianchi, A., Larmola, T., Kekkonen, H., Saarnio, S., Lång, K., 2021. Review of Greenhouse
759 Gas Emissions from Rewetted Agricultural Soils. *Wetlands* 2021 41:8 41, 108-.
760 <https://doi.org/10.1007/S13157-021-01507-5>

761 Bonaglia, S., Cheung, H.L.S., Politi, T., Vybernaite-Lubiene, I., McKenzie, T., Santos, I.R.,
762 Zilius, M., 2025. Eutrophication and urbanization enhance methane emissions from
763 coastal lagoons. *Limnol Oceanogr Lett* 10, 140–150.
764 <https://doi.org/10.1002/lol2.10430>

765 Cabrera-Brufau, M., Minaudo, C., von Schiller, D., Obrador, B., Attermeyer, K., Camacho, A.,
766 2025. Instantaneous fluxes of carbon dioxide (CO₂) and methane (CH₄) of six
767 European coastal wetlands under different ecological status measured seasonally
768 with static chambers [Data set]. LifeWatch ERIC. <https://doi.org/10.48372/C29B-QW38>

769

770 Camacho, A., Picazo, A., Rochera, C., Santamans, A., Morant, D., Miralles-Lorenzo, J.,
771 Castillo-Escrivà, A., 2017. Methane Emissions in Spanish Saline Lakes: Current Rates,
772 Temperature and Salinity Responses, and Evolution under Different Climate Change
773 Scenarios. *Water (Basel)* 9, 659. <https://doi.org/10.3390/w9090659>

774 Camacho-Santamans, A., Morant, D., Rochera, C., Picazo, A., Camacho, A., 2025. Towards
775 an enhancement of the climate change mitigation capacity of inland saline shallow
776 lakes through hydrological regime and vegetation management: a modelling
777 approach. *Water Int* 50, 197–224. <https://doi.org/10.1080/02508060.2024.2311997>

778 Canadell, J.G., Monteiro, P.M.S., 2023. Global Carbon and Other Biogeochemical Cycles
779 and Feedbacks, in: *Climate Change 2021 – The Physical Science Basis*. Cambridge
780 University Press, pp. 673–816. <https://doi.org/10.1017/9781009157896.007>

781 Cui, S., Liu, P., Guo, H., Nielsen, C.K., Pullens, J.W.M., Chen, Q., Pugliese, L., Wu, S., 2024.
782 Wetland hydrological dynamics and methane emissions. *Communications Earth &*
783 *Environment* 2024 5:1 5, 470-. <https://doi.org/10.1038/s43247-024-01635-w>

784 Davidson, I.C., Cott, G.M., Devaney, J.L., Simkanin, C., 2018. Differential effects of
785 biological invasions on coastal blue carbon: A global review and meta-analysis. *Glob
786 Chang Biol* 24, 5218–5230. <https://doi.org/10.1111/gcb.14426>

787 European Environment Agency, 2024. Europe's state of water 2024 – The need for improved
788 water resilience. Publications Office of the European Union.
789 <https://doi.org/doi/10.2800/02236>

790 European Union, 2024. Regulation (EU) 2024/1991 of the European Parliament and of the
791 Council of 24 June 2024 on nature restoration and amending Regulation (EU)
792 2022/869.

793 Fluet-Chouinard, E., Stocker, B.D., Zhang, Z., Malhotra, A., Melton, J.R., Poulter, B., Kaplan,
794 J.O., Goldewijk, K.K., Siebert, S., Minayeva, T., Hugelius, G., Joosten, H., Barthelmes,
795 A., Prigent, C., Aires, F., Hoyt, A.M., Davidson, N., Finlayson, C.M., Lehner, B., Jackson,
796 R.B., McIntyre, P.B., 2023. Extensive global wetland loss over the past three centuries.
797 *Nature* 2023 614:7947 614, 281–286. <https://doi.org/10.1038/s41586-022-05572-6>

798 Ge, M., Korrensalo, A., Laiho, R., Kohl, L., Lohila, A., Pihlatie, M., Li, X., Laine, A.M., Anttila,
799 J., Putkinen, A., Wang, W., Koskinen, M., 2024. Plant-mediated CH₄ exchange in
800 wetlands: A review of mechanisms and measurement methods with implications for
801 modelling. *Science of the Total Environment*.
802 <https://doi.org/10.1016/j.scitotenv.2023.169662>

803 Graves, S., Piepho, H.-P., with help from Sundar Dorai-Raj, L.S., 2024. *multcompView:*
804 *Visualizations of Paired Comparisons*.
805 <https://doi.org/10.32614/CRAN.package.multcompView>

806 Griscom, B.W., Adams, J., Ellis, P.W., Houghton, R.A., Lomax, G., Miteva, D.A., Schlesinger,
807 W.H., Shoch, D., Siikamäki, J. V., Smith, P., Woodbury, P., Zganjar, C., Blackman, A.,
808 Campari, J., Conant, R.T., Delgado, C., Elias, P., Gopalakrishna, T., Hamsik, M.R.,
809 Herrero, M., Kiesecker, J., Landis, E., Laestadius, L., Leavitt, S.M., Minnemeyer, S.,
810 Polasky, S., Potapov, P., Putz, F.E., Sanderman, J., Silvius, M., Wollenberg, E., Fargione,
811 J., 2017. Natural climate solutions. *Proceedings of the National Academy of Sciences*
812 114, 11645–11650. <https://doi.org/10.1073/pnas.1710465114>

813 Hartig, F., 2024. DHARMA: Residual Diagnostics for Hierarchical (Multi-Level /
814 Mixed) Regression Models. <https://doi.org/10.32614/CRAN.package.DHARMA>

815 He, T., Ding, W., Cheng, X., Cai, Y., Zhang, Y., Xia, H., Wang, X., Zhang, J., Zhang, K., Zhang,
816 Q., 2024. Meta-analysis shows the impacts of ecological restoration on greenhouse
817 gas emissions. *Nat Commun* 15, 2668. <https://doi.org/10.1038/s41467-024-46991-5>

818 Hutchinson, G.L., Mosier, A.R., 1981. Improved Soil Cover Method for Field Measurement
819 of Nitrous Oxide Fluxes. *Soil Science Society of America Journal* 45, 311–316.
820 <https://doi.org/10.2136/sssaj1981.03615995004500020017x>

821 IPCC, 2023. *Climate Change 2021 – The Physical Science Basis*. Cambridge University
822 Press, Cambridge. <https://doi.org/10.1017/9781009157896>

823 Jones, S.F., Arias-Ortiz, A., Baldocchi, D., Eagle, M., Friess, D.A., Gore, C., Noe, G., Nolte, S.,
824 Oikawa, P., Paytan, A., Raw, J.L., Roberts, B.J., Rogers, K., Schutte, C., Stagg, C.L.,
825 Thorne, K.M., Ward, E.J., Windham-Myers, L., Yando, E.S., 2024. When and where can
826 coastal wetland restoration increase carbon sequestration as a natural climate
827 solution? *Cambridge Prisms: Coastal Futures*. <https://doi.org/10.1017/cft.2024.14>

828 Kasak, K., Espenberg, M., Anthony, T.L., Tringe, S.G., Valach, A.C., Hemes, K.S., Silver, W.L.,
829 Mander, Ü., Kill, K., McNicol, G., Szutu, D., Verfaillie, J., Baldocchi, D.D., 2021.
830 Restoring wetlands on intensive agricultural lands modifies nitrogen cycling microbial

831 communities and reduces N₂O production potential. *J Environ Manage* 299, 113562.
832 <https://doi.org/10.1016/J.JENVMAN.2021.113562>

833 Koebsch, F., Winkel, M., Liebner, S., Liu, B., Westphal, J., Schmiedinger, I., Spitz, A., Gehre,
834 M., Jurasic, G., Köhler, S., Unger, V., Koch, M., Sachs, T., Böttcher, M.E., 2019.
835 Sulfate deprivation triggers high methane production in a disturbed and rewetted
836 coastal peatland. *Biogeosciences* 16, 1937–1953. <https://doi.org/10.5194/BG-16-1937-2019>

838 Lenth, R. V., 2025. emmeans: Estimated Marginal Means, aka Least-Squares Means.
839 <https://doi.org/10.32614/CRAN.package.emmeans>

840 Leo, K.L., Gillies, C.L., Fitzsimons, J.A., Hale, L.Z., Beck, M.W., 2019. Coastal habitat
841 squeeze: A review of adaptation solutions for saltmarsh, mangrove and beach
842 habitats. *Ocean Coast Manag* 175, 180–190.
843 <https://doi.org/10.1016/J.OCECOAMAN.2019.03.019>

844 Lin, C.W., Lin, W.J., Ho, C.W., Kao, Y.C., Yong, Z.J., Lin, H.J., 2024. Flushing emissions of
845 methane and carbon dioxide from mangrove soils during tidal cycles. *Science of The
846 Total Environment* 919, 170768. <https://doi.org/10.1016/J.SCITOTENV.2024.170768>

847 Lorke, A., Bodmer, P., Noss, C., Alshboul, Z., Koschorreck, M., Somlai-Haase, C., Bastviken,
848 D., Flury, S., McGinnis, D.F., Maeck, A., Müller, D., Premke, K., 2015. Technical note:
849 drifting versus anchored flux chambers for measuring greenhouse gas emissions from
850 running waters. *Biogeosciences* 12, 7013–7024. <https://doi.org/10.5194/bg-12-7013-2015>

852 Lovley, D.R., Klug, M.J., 1983. Sulfate reducers can outcompete methanogens at freshwater
853 sulfate concentrations. *Appl Environ Microbiol* 45, 187–192.
854 [https://doi.org/10.1128/AEM.45.1.187-192.1983;WGROU:STRING:PUBLICATI](https://doi.org/10.1128/AEM.45.1.187-192.1983)

855 Macreadie, P.I., Anton, A., Raven, J.A., Beaumont, N., Connolly, R.M., Friess, D.A., Kelleway,
856 J.J., Kennedy, H., Kuwae, T., Lavery, P.S., Lovelock, C.E., Smale, D.A., Apostolaki, E.T.,
857 Atwood, T.B., Baldock, J., Bianchi, T.S., Chmura, G.L., Eyre, B.D., Fourqurean, J.W.,
858 Hall-Spencer, J.M., Huxham, M., Hendriks, I.E., Krause-Jensen, D., Laffoley, D.,
859 Luisetti, T., Marbà, N., Masque, P., McGlathery, K.J., Megonigal, J.P., Murdiyarno, D.,
860 Russell, B.D., Santos, R., Serrano, O., Silliman, B.R., Watanabe, K., Duarte, C.M., 2019.
861 The future of Blue Carbon science. *Nat Commun* 10, 3998.
862 <https://doi.org/10.1038/s41467-019-11693-w>

863 Maes, J., Teller, A., Erhard, M., Condé, S., Vallecillo, S., Barredo, J.I., Luisa, M., Malak, D.A.,
864 Trombetti, M., Vigiak, O., Zulian, G., Addamo, A.M., Grizzetti, B., Somma, F., Hagyo, A.,
865 Vogt, P., Polce, C., Jones, A., Marin, A.I., Ivits, E., Mauri, A., Rega, C., Czucz, B.,
866 Ceccherini, G., Pisoni, E., Ceglar, A., Palma, P. De, Cerrani, I., Meroni, M., Caudullo, G.,
867 Lugato, E., Vogt, J. V., Spinoni, J., Cammalleri, C., Bastrup-birk, A., Miguel, J.S., Román,
868 S.S., Kristensen, P., Christiansen, T., Roo, A. De, Cardoso, A.C., Pistocchi, A., Del, I.,
869 Alvarellos, B., Tsiamis, K., Gervasini, E., Deriu, I., Notte, A. La, Viñas, R.A., Vizzarri, M.,
870 Camia, A., Kakoulaki, G., Bendito, E.G., Panagos, P., Ballabio, C., Scarpa, S., Orgiazzi,
871 A., Ugalde, O.F., Santos-martín, F., 2020. Mapping and Assessment of Ecosystems and
872 their Services : An EU ecosystem assessment. <https://doi.org/10.2760/757183>

873 Maier, M., Weber, T.K.D., Fiedler, J., Fuß, R., Glatzel, S., Huth, V., Jordan, S., Jurasinski, G.,
874 Kutzbach, L., Schäfer, K., Weymann, D., Hagemann, U., 2022. Introduction of a
875 guideline for measurements of greenhouse gas fluxes from soils using non-steady-
876 state chambers. *Journal of Plant Nutrition and Soil Science* 185, 447–461.
877 <https://doi.org/10.1002/JPLN.202200199>

878 McGillycuddy, M., Warton, D.I., Popovic, G., Bolker, B.M., 2025. Parsimoniously Fitting Large
879 Multivariate Random Effects in glmmTMB. *J Stat Softw* 112, 1–19.
880 <https://doi.org/10.18637/jss.v112.i01>

881 Meli, P., Benayas, J.M.R., Balvanera, P., Ramos, M.M., 2014. Restoration Enhances Wetland
882 Biodiversity and Ecosystem Service Supply, but Results Are Context-Dependent: A
883 Meta-Analysis. *PLoS One* 9, e93507.
884 <https://doi.org/10.1371/JOURNAL.PONE.0093507>

885 Minaudo, C., Cabrera-Brufau, M., Montes-Pérez, J.J., Attermeyer, K., Camacho, A.,
886 Camacho-Santamans, A., Cazacu, C., Giuca, R., Lillebø, A., Misteli, B., Morant, D.,
887 Obrador, B., Oliveira, B., Petkuvienė, J., Picazo, A., Rochera, C., von Schiller, D., 2025.
888 Uncertainty in aquatic greenhouse gas flux estimates arises from subjective
889 processing of floating chamber time series. *EarthArXiv* preprint.
890 <https://doi.org/10.31223/X5MN29>

891 Minaudo, C., von Schiller, D., Misteli, B., Morant, D., Adamescu, M., Attermeyer, K., Basset,
892 A., Carballeira, R., Cazacu, C., Coelho, J.P., Guelmami, A., Hilaire, S., Miralles, J.,
893 Obrador, B., Petkuviene, J., Picazo, A., Rochera, C., Santinelli, C., Teixeira, H., Titocci,
894 J., Vaicute, D., Camacho, A., 2023. Methodological manual. Deliverable D4.2 Horizon
895 RESTORE4Cs Project GA ID: 101056782.

896 Miralles-Lorenzo, J., Picazo, A., Rochera, C., Morant, D., Casamayor, E.O., Menéndez-Serra,
897 M., Camacho, A., 2025. Environmental Gradients and Conservation Status Determine
898 the Structure and Carbon-Related Metabolic Potential of the Prokaryotic Communities
899 of Mediterranean Inland Saline Shallow Lakes. *Ecol Evol* 15, e71286.
900 <https://doi.org/10.1002/ece3.71286>

901 Misteli, B., Morant, D., Camacho, A., Adamo, M., Bachi, G., Bègue, N., Bučas, M., Cabrera-
902 Brufau, M., Carballeira, R., Cavalcante, L., Cazacu, C., Coelho, J., Doebke, C., Dinu, V.,
903 Guelmami, A., Giuca, R., Kataržytė, M., Lillebø, A., Marin, A., Marangi, C., Minaudo, C.,
904 Montes-Pérez, J., Obrador, B., Oliveira, B., Petkuvienė, J., Picazo, A., van Puijenbroek,
905 M., Ronse, M., Rochera, C., Sánchez, A., Santinelli, C., Sousa, A., von Schiller, D.,
906 Attermeyer, K., Tropea, C., Vaičiūtė, D., 2025. Coastal Wetland Restoration and
907 Greenhouse Gas Pathways: A Global Meta-Analysis. *EarthArXiv* preprint.
908 <https://doi.org/10.31223/X51B39>

909 Mitsch, W.J., Bernal, B., Nahlik, A.M., Mander, Ü., Zhang, L., Anderson, C.J., Jørgensen, S.E.,
910 Brix, H., 2012. Wetlands, carbon, and climate change. *Landscape Ecology* 2012 28:4
911 28, 583–597. <https://doi.org/10.1007/S10980-012-9758-8>

912 Morant, D., Picazo, A., Rochera, C., Santamans, A.C., Miralles-Lorenzo, J., Camacho, A.,
913 2020a. Influence of the conservation status on carbon balances of semiarid coastal
914 Mediterranean wetlands. *Inland Waters* 10, 453–467.
915 <https://doi.org/10.1080/20442041.2020.1772033>

916 Morant, D., Picazo, A., Rochera, C., Santamans, A.C., Miralles-Lorenzo, J., Camacho-
917 Santamans, A., Ibañez, C., Martínez-Eixarch, M., Camacho, A., 2020b. Carbon
918 metabolic rates and GHG emissions in different wetland types of the Ebro Delta. PLoS
919 One 15, e0231713. <https://doi.org/10.1371/journal.pone.0231713>

920 Morant, D., Rochera, C., Picazo, A., Miralles-Lorenzo, J., Camacho-Santamans, A.,
921 Camacho, A., 2024. Ecological status and type of alteration determine the C-balance
922 and climate change mitigation capacity of Mediterranean inland saline shallow lakes.
923 Sci Rep 14, 29065. <https://doi.org/10.1038/s41598-024-79578-7>

924 Moreno-Mateos, D., Barbier, E.B., Jones, P.C., Jones, H.P., Aronson, J., López-López, J.A.,
925 McCrackin, M.L., Meli, P., Montoya, D., Rey Benayas, J.M., 2017. Anthropogenic
926 ecosystem disturbance and the recovery debt. Nature Communications 2017 8:1 8,
927 14163-. <https://doi.org/10.1038/ncomms14163>

928 Moreno-Mateos, D., Power, M.E., Comín, F.A., Yockteng, R., 2012. Structural and Functional
929 Loss in Restored Wetland Ecosystems. PLoS Biol 10, e1001247.
930 <https://doi.org/10.1371/JOURNAL.PBIO.1001247>

931 Neubauer, S.C., 2021. Global Warming Potential Is Not an Ecosystem Property. Ecosystems
932 2021 24:8 24, 2079–2089. <https://doi.org/10.1007/S10021-021-00631-X>

933 O'Connor, J.J., Fest, B.J., Sievers, M., Swearer, S.E., 2020. Impacts of land management
934 practices on blue carbon stocks and greenhouse gas fluxes in coastal ecosystems—A
935 meta-analysis. Glob Chang Biol 26, 1354–1366. <https://doi.org/10.1111/gcb.14946>

936 Oliveira, R.B., Camacho, A., Guelmami, A., Schroder, C., Bègue, N., Bučas, M., Cazacu, C.,
937 Ciravegna, E., Coelho, J.P., Relu Giuca, C., Hilaire, S., Kataržyté, M., Morant, D., Picazo,
938 A., Polman, N., van Puijenbroek, M., Raoult, J., Rochera, C., Ronse, M., Sella, L., Sousa,
939 A.I., Racoviceanu, T., Rota, F.S., Vaičiūtė, D., Lillebø, A.I., n.d. (Submitted) European
940 coastal wetlands datasets and their use in decision-support tools for policy
941 restoration objectives. Environmental Science and Policy (Under review).

942 Palmer, M.A., Zedler, J.B., Falk, D.A., 2016. Ecological Theory and Restoration Ecology.
943 Foundations of Restoration Ecology: Second Edition 3–26.
944 https://doi.org/10.5822/978-1-61091-698-1_1

945 Peterson, R.A., 2021. Finding Optimal Normalizing Transformations via bestNormalize. R J
946 13, 310–329. <https://doi.org/10.32614/RJ-2021-041>

947 Pörtner, H.-O., Scholes, R.J., Agard, J., Archer, E., Arneth, A., Bai, X., Barnes, D., Burrows,
948 M., Chan, L., Cheung, W.L. (William), Diamond, S., Donatti, C., Duarte, C., Eisenhauer,
949 N., Foden, W., Gasalla, M.A., Handa, C., Hickler, T., Hoegh-Guldberg, O., Ichii, K.,
950 Jacob, U., Insarov, G., Kiessling, W., Leadley, P., Leemans, R., Levin, L., Lim, M.,
951 Maharaj, S., Managi, S., Marquet, P.A., McElwee, P., Midgley, G., Oberdorff, T., Obura,
952 D., Osman Elasha, B., Pandit, R., Pascual, U., Pires, A.P.F., Popp, A., Reyes-García, V.,
953 Sankaran, M., Settele, J., Shin, Y.-J., Sintayehu, D.W., Smith, P., Steiner, N., Strassburg,
954 B., Sukumar, R., Trisos, C., Val, A.L., Wu, J., Aldrian, E., Parmesan, C., Pichs-Madruga,
955 R., Roberts, D.C., Rogers, A.D., Díaz, S., Fischer, M., Hashimoto, S., Lavorel, S., Wu, N.,
956 Ngo, H., 2021. Scientific outcome of the IPBES-IPCC co-sponsored workshop on
957 biodiversity and climate change. <https://doi.org/10.5281/ZENODO.5101125>

958 R Core Team, 2025. R: A Language and Environment for Statistical Computing.

959 Ramsar Convention, 1971. Convention on Wetlands of International Importance especially
960 as Waterfowl Habitat. Ramsar.

961 Reddy, K.R., DeLaune, R.D., Inglett, P.W., 2022. Biogeochemistry of Wetlands : Science and
962 Applications. Biogeochemistry of Wetlands. <https://doi.org/10.1201/9780429155833>

963 Regnier, P., Resplandy, L., Najjar, R.G., Ciais, P., 2022. The land-to-ocean loops of the global
964 carbon cycle. *Nature* 2022 603:7901 603, 401–410. <https://doi.org/10.1038/s41586-021-04339-9>

966 Remeikaite-Nikiene, N., Lujaniene, G., Malejevas, V., Barisevičiute, R., Žilius, M., Garnaga-
967 Budre, G., Stankevičius, A., 2016. Distribution and sources of organic matter in
968 sediments of the south-eastern Baltic Sea. *Journal of Marine Systems* 157, 75–81.
969 <https://doi.org/10.1016/J.JMARSYS.2015.12.011>

970 Rheault, K., Christiansen, J.R., Larsen, K.S., 2024. goFlux: A user-friendly way to calculate
971 GHG fluxes yourself, regardless of user experience. *J Open Source Softw* 9, 6393.
972 <https://doi.org/10.21105/joss.06393>

973 Rissanen, A.J., Jilbert, T., Simojoki, A., Mangayil, R., Aalto, S.L., Khanongnuch, R., Peura, S.,
974 Jäntti, H., 2023. Organic matter lability modifies the vertical structure of methane-
975 related microbial communities in lake sediments. *Microbiol Spectr* 11.
976 <https://doi.org/10.1128/spectrum.01955-23>

977 Rochera, C., Picazo, A., Morant, D., Miralles-Lorenzo, J., Sánchez-Ortega, V., Camacho, A.,
978 2025a. Linking Carbon Fluxes to Flooding Gradients in Sediments of Mediterranean
979 Wetlands. *ACS ES&T Water* 5, 2882–2890.
980 <https://doi.org/10.1021/acsestwater.4c00940>

981 Rochera, C., Picazo, A., Morant, D., Miralles-Lorenzo, J., Sánchez-Ortega, V., Camacho, A.,
982 2025b. Linking Carbon Fluxes to Flooding Gradients in Sediments of Mediterranean
983 Wetlands. *ACS ES&T Water* 5, 2882–2890.
984 <https://doi.org/10.1021/ACSESTWATER.4C00940>

985 Romm, J., Lezak, S., Alshamsi, A., 2025. Are Carbon Offsets Fixable? *Annu Rev Environ*
986 *Resour* 50, 649–680. <https://doi.org/10.1146/annurev-environ-112823-064813>

987 Rosentreter, J.A., Al-Haj, A.N., Fulweiler, R.W., Williamson, P., 2021. Methane and Nitrous
988 Oxide Emissions Complicate Coastal Blue Carbon Assessments. *Global Biogeochem*
989 *Cycles* 35, e2020GB006858. <https://doi.org/10.1029/2020GB006858>

990 Saunois, M., Bousquet, P., Poulter, B., Pergon, A., Ciais, P., Canadell, J.G., Dlugokencky,
991 E.J., Etiope, G., Bastviken, D., Houweling, S., Janssens-Maenhout, G., Tubiello, F.N.,
992 Castaldi, S., Jackson, R.B., Alexe, M., Arora, V.K., Beerling, D.J., Bergamaschi, P., Blake,
993 D.R., Brailsford, G., Brovkin, V., Bruhwiler, L., Crevoisier, C., Crill, P., Covey, K., Curry,
994 C., Frankenberg, C., Gedney, N., Höglund-Isaksson, L., Ishizawa, M., Ito, A., Joos, F.,
995 Kim, H.S., Kleinen, T., Krummel, P., Lamarque, J.F., Langenfelds, R., Locatelli, R.,
996 Machida, T., Maksyutov, S., McDonald, K.C., Marshall, J., Melton, J.R., Morino, I., Naik,
997 V., O'Doherty, S., Parmentier, F.J.W., Patra, P.K., Peng, C., Peng, S., Peters, G.P., Pison,
998 I., Prigent, C., Prinn, R., Ramonet, M., Riley, W.J., Saito, M., Santini, M., Schroeder, R.,
999 Simpson, I.J., Spahni, R., Steele, P., Takizawa, A., Thornton, B.F., Tian, H., Tohjima, Y.,

1000 Viovy, N., Voulgarakis, A., Van Weele, M., Van Der Werf, G.R., Weiss, R., Wiedinmyer,
1001 C., Wilton, D.J., Wiltshire, A., Worthy, D., Wunch, D., Xu, X., Yoshida, Y., Zhang, B.,
1002 Zhang, Z., Zhu, Q., 2016. The global methane budget 2000-2012. *Earth Syst Sci Data* 8,
1003 697-751. <https://doi.org/10.5194/ESSD-8-697-2016>

1004 Schorn, S., Ahmerkamp, S., Bullock, E., Weber, M., Lott, C., Liebeke, M., Lavik, G., Kuypers,
1005 M.M.M., Graf, J.S., Milucka, J., 2022. Diverse methylotrophic methanogenic archaea
1006 cause high methane emissions from seagrass meadows. *Proc Natl Acad Sci U S A* 119.
1007 <https://doi.org/10.1073/PNAS.2106628119/-/DCSUPPLEMENTAL>

1008 Schuster, L., Taillardat, P., Macreadie, P.I., Malerba, M.E., 2024. Freshwater wetland
1009 restoration and conservation are long-term natural climate solutions. *Science of The
1010 Total Environment* 922, 171218. <https://doi.org/10.1016/j.scitotenv.2024.171218>

1011 Singh, N.K., Gourevitch, J.D., Wemple, B.C., Watson, K.B., Rizzo, D.M., Polasky, S., Ricketts,
1012 T.H., 2019. Optimizing wetland restoration to improve water quality at a regional scale.
1013 *Environmental Research Letters* 14, 064006. <https://doi.org/10.1088/1748-9326/AB1827>

1015 Suding, K.N., Gross, K.L., Houseman, G.R., 2004. Alternative states and positive feedbacks
1016 in restoration ecology. *Trends Ecol Evol* 19, 46-53.
1017 <https://doi.org/10.1016/j.tree.2003.10.005>

1018 Taillardat, P., Thompson, B.S., Garneau, M., Trottier, K., Friess, D.A., 2020. Climate change
1019 mitigation potential of wetlands and the cost-effectiveness of their restoration.
1020 *Interface Focus* 10, 20190129. <https://doi.org/10.1098/rsfs.2019.0129>

1021 Thieurmel, B., Elmarhraoui, A., 2022. *suncalc*: Compute Sun Position, Sunlight Phases,
1022 Moon Position and Lunar Phase. <https://doi.org/10.32614/CRAN.package.suncalc>

1023 Vaičiūtė, D., Bučas, M., Bresciani, M., Dabulevičienė, T., Gintauskas, J., Méžinė, J., Tiškus,
1024 E., Umgiesser, G., Morkūnas, J., De Santi, F., Bartoli, M., 2021. Hot moments and
1025 hotspots of cyanobacteria hyperblooms in the Curonian Lagoon (SE Baltic Sea)
1026 revealed via remote sensing-based retrospective analysis. *Science of The Total
1027 Environment* 769, 145053. <https://doi.org/10.1016/j.scitotenv.2021.145053>

1028 Ward, S.E., Bardgett, R.D., McNamara, N.P., Ostle, N.J., 2009. Plant functional group identity
1029 influences short-term peatland ecosystem carbon flux: evidence from a plant removal
1030 experiment. *Funct Ecol* 23, 454-462. <https://doi.org/10.1111/J.1365-2435.2008.01521.X>

1032 Wickham, H., 2016. *ggplot2: Elegant Graphics for Data Analysis*. Springer-Verlag New York.

1033 Wickham, H., Pedersen, T.L., Seidel, D., 2025. *scales: Scale Functions for Visualization*.
1034 <https://doi.org/10.32614/CRAN.package.scales>

1035 Wu, Y., Sun, J., Hu, B., Zhang, G., Rousseau, A.N., 2023. Wetland-based solutions against
1036 extreme flood and severe drought: Efficiency evaluation of risk mitigation. *Clim Risk
1037 Manag* 40, 100505. <https://doi.org/10.1016/J.CRM.2023.100505>

1038 Zilius, M., Bartoli, M., Bresciani, M., Katarzyte, M., Ruginis, T., Petkuviene, J., Lubiene, I.,
1039 Giardino, C., Bukaveckas, P.A., de Wit, R., Razinkovas-Baziukas, A., 2013. Feedback
1040 Mechanisms Between Cyanobacterial Blooms, Transient Hypoxia, and Benthic

1041 Phosphorus Regeneration in Shallow Coastal Environments. *Estuaries and Coasts*
1042 2013 37:3 37, 680–694. <https://doi.org/10.1007/S12237-013-9717-X>

1043 Zorrilla-Miras, P., Palomo, I., Gómez-Baggethun, E., Martín-López, B., Lomas, P.L., Montes,
1044 C., 2014. Effects of land-use change on wetland ecosystem services: A case study in
1045 the Doñana marshes (SW Spain). *Landsc Urban Plan* 122, 160–174.
1046 <https://doi.org/10.1016/J.LANDURBPLAN.2013.09.013>

1047

1048

1049 **Supplementary materials**

1050 **1. Detailed description of European case pilot wetlands**

1051 *South-West Dutch Delta (DU)*

1052 Preserved sites consisted of Intertidal salt marshes showing natural hydrological and
1053 sedimentation processes, vegetated surfaces, and minimal disruption by coastal
1054 infrastructure. These sites maintained natural marsh integrity and ecological processes
1055 including tidal inundation patterns, natural sedimentation, pioneer zone species, and mid-
1056 upper marsh communities. The main alterations were the installation of stone breakwaters
1057 or wooden pales perpendicular to the marsh to reduce hydrodynamics and locally reduce
1058 erosion. These hard structures disrupted natural sedimentation processes and reflected
1059 wave energy, leading to accelerated lateral erosion and creek widening, prevention of
1060 natural landward marsh development and disappearance of pioneer-zone plant species.
1061 Restoration involved morphological reconstruction and recovery of natural hydrodynamics
1062 through managed realignment. In both cases, the displacement of the coastal defense line
1063 further inland facilitated recovery of natural hydrodynamics, tidal patterns, sedimentation
1064 processes, and vegetation establishment on previously reclaimed land.

1065 *Ria de Aveiro (RI)*

1066 Preserved sites exhibited healthy intertidal seagrass meadows with high coverage of
1067 *Zostera noltii*, stable sediment structure, and absence of significant anthropogenic
1068 pressures. The main alteration consisted of erosion and bioturbation from bait-digging
1069 activities and physical disturbance from trampling. Altered sites consist of bare,
1070 unvegetated intertidal areas where meadows have been lost or severely degraded. These
1071 areas exhibit high erosion, unstable sediments prone to resuspension and reduced
1072 biodiversity. Restoration actions consisted of re-vegetation: Active mosaic-pattern
1073 transplantation of *Z. noltii* have been formerly performed in zones where pressures are no
1074 longer relevant. Transplants were able to cover previously unvegetated areas and develop
1075 uniform, robust coverage throughout the restored sites within one year.

1076 *Camargue (CA)*

1077 Preserved sites were selected from mediterranean freshwater marshes and ponds that
1078 retained natural hydrological regimes and ecological features, without significant historical
1079 land use conversion or hydrological alterations. These sites maintained intact soil and
1080 seasonal flooding and drying patterns characteristic of Mediterranean freshwater wetlands,
1081 supporting native flora and fauna. This case pilot suffered mainly from hydrological, trophic,
1082 and land-use change impacts. The altered sites included former fishponds and areas that
1083 had been subjected to decades of artificial hydrological regimes, mainly favoring hunting
1084 activities. These sites experienced hydrological alterations driven by artificial irrigation and
1085 drainage systems, leading to long-term changes in water regimes. The natural seasonal
1086 hydrological variability was replaced by highly managed water regimes, with continuous
1087 flooding during dry seasons. Restoration activities involved soil, hydrology, vegetation and
1088 morphological reconstruction of former rice fields and pastures. Topographic reshaping,
1089 removal of drainage and irrigation infrastructure, soil and seed transfers allowed for the
1090 recovery of natural flooding and drying cycles, recolonization by native wetland vegetation
1091 and increasing presence of amphibians and waterbirds in the sites.

1092 *Valencian wetland Marjal dels Moros (VA)*

1093 The selected preserved sites were coastal brackish marshes with intact emergent swamp
1094 communities, natural hydrological connectivity, and limited structural and water quality
1095 degradation. These areas featured native plant communities adapted to brackish
1096 conditions (reeds, bulrush stands and halophytic shrubs) and natural hydrodynamics
1097 controlled by precipitation, evaporation and seawater intrusion via groundwater. This
1098 wetland suffers mostly from hydrological, trophic, and morphological alterations. The
1099 representative altered sites are subject to artificial water supply from irrigation and
1100 wastewater sources as well as morphological modification (land-use change and soil
1101 degradation). These pressures resulted in areas with reduced native vegetation and
1102 proliferation of invasive species, and degraded water quality with elevated nutrients and
1103 loss of characteristic brackish conditions due to desalinization. As restored sites, areas
1104 were selected where various actions were performed. Active restoration included soil
1105 reconstruction to improve substrate conditions, morphological reconstruction of natural
1106 topology and hydrological connectivity, and planting of native vegetation. Hydrological
1107 actions ensure diverse good-quality water sources to maintain aquatic refuges for fauna via
1108 flood regulation while maintaining characteristic brackish conditions. Mowing of helophytic
1109 vegetation is regularly implemented to maintain habitat heterogeneity.

1110 *Danube Delta (DA)*

1111 Preserved sites consisted of freshwater shallow lakes with native submerged (*Potamogeton*
1112 spp., *Ceratophyllum* spp.) and floating vegetation (*Trapa natans* L., *Nymphaea alba* L.)
1113 surrounded by reed beds (*Phragmites australis* L.). These sites lacked major anthropogenic
1114 pressures, maintained their connectivity to the river network and are classified as having
1115 good ecological status according to the Water Framework Directive. The most relevant
1116 impacts of this pilot are hydrological and morphological alterations related to land-use
1117 change. Altered sites were former freshwater wetlands converted to dryland during the
1118 1980s. One site consisted of an agricultural field used to grow cereal. The other site was
1119 initially used for pasture for cattle but was flooded due to dike failure and was subsequently
1120 abandoned for this use. These areas suffered lack of native vegetation, soil alteration and
1121 high nutrient loads from fertilizers and manure, respectively. Restoration activities
1122 consisted of the morphological and hydrological reconstruction of wetland habitats from
1123 former pastures and degraded wetlands. Restoration of sites involved the recovery of
1124 natural hydrological regimes via their re-connection to the river network and flood
1125 management via pumping stations, as well as the removal of excess reed cover to create
1126 open water habitats.

1127 *Curonian Lagoon (CU)*

1128 Preserved sites consisted of littoral zones characterized by high coverage of submerged
1129 aquatic vegetation (*Chara contraria*, *Chara apsera*, *Chara globularis*, *Potamogeton*
1130 *perfoliatus*, *Stuckenia pectinata*), with sandy or mixed bottom substrates and emergent
1131 reeds (*P. Australis*). The relatively low nutrient loads and chlorophyll-a concentrations of
1132 these areas are characteristic of balanced trophic conditions in the Lagoon. The most
1133 relevant pressures within the system consist of eutrophication and organic matter
1134 enrichment. Altered trophic state is driven by high nutrient loads from agricultural runoff
1135 and insufficient wastewater treatment from the Neumas river. The altered sites selected
1136 were characterized by elevated nutrient levels and associated high chlorophyll-a
1137 concentrations with episodic cyanobacterial blooms. The accumulation of organic-rich

1138 mud in the substrate promotes anoxic conditions and leads to a reduction in submerged
1139 aquatic vegetation. Restoration actions at the watershed level aimed at improving water
1140 quality and local-scale measures, such as reed harvesting to reduce excess nutrients and
1141 organic matter. Improvements of wastewater treatment infrastructure and reduced fertilizer
1142 use in the upstream Nemunas river basin led to reduced nutrient loads. In addition,
1143 hydrological changes such as increased brackish water intrusions due to the artificial
1144 deepening of the Klaipéda Strait channel (Stakénienė et al., 2023) and decreased annual
1145 runoff from the Nemunas River (Idzelyte- et al., 2023) have likely reduced fine sediment
1146 inputs and muddy sediment accumulation. These changes have affected recovery of sandy
1147 sediment areas and promoted the expansion of submerged aquatic vegetation in restored
1148 sites.

1149 2. Best-flux estimate selection

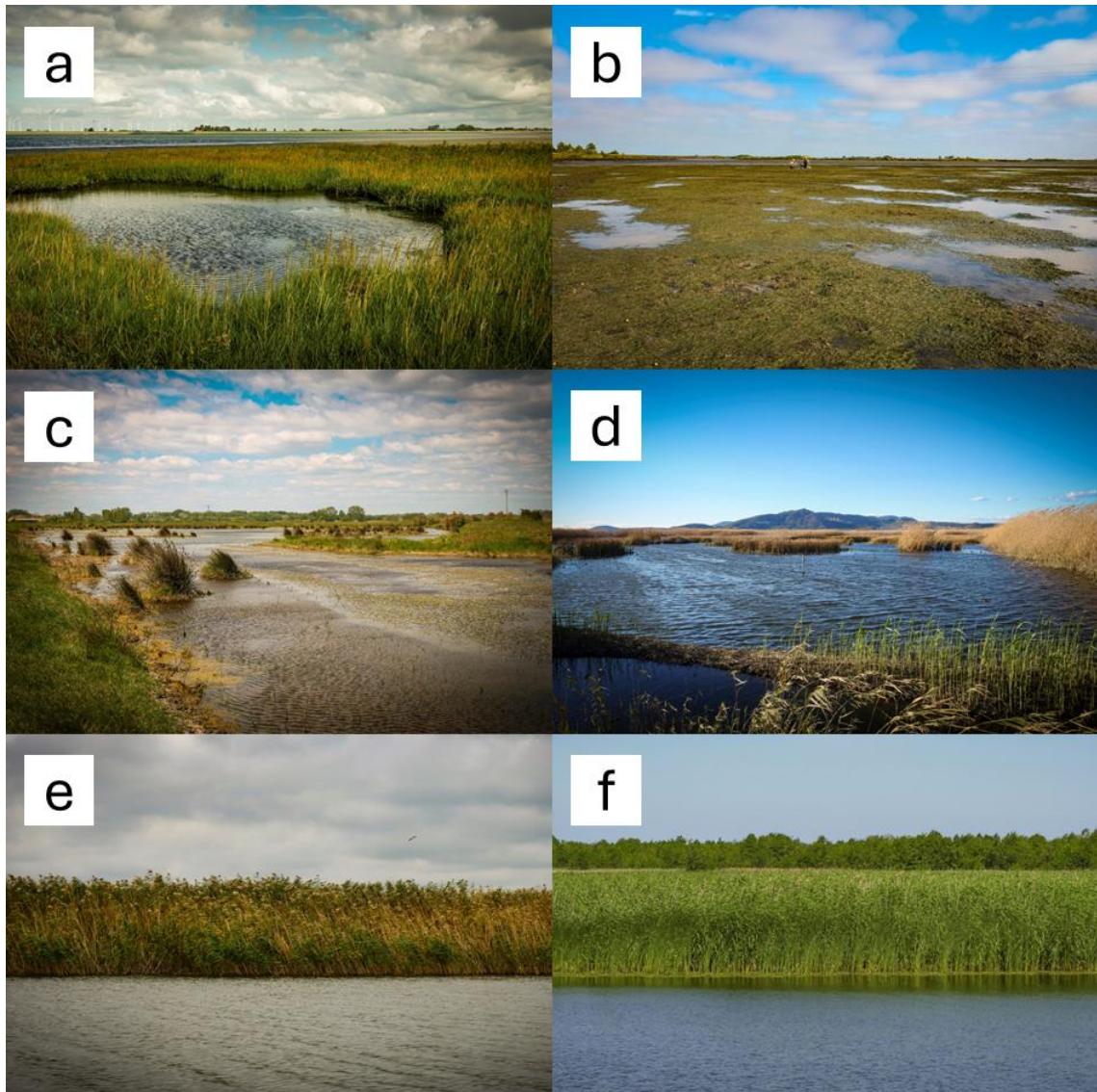
1150 A common set of sequential criteria was followed to select a best-flux estimate from those
1151 produced by the three models: two-point, linear model (LM) and a non-linear (HM)
1152 (Hutchinson & Mosier, 1981) regression model. Choosing an appropriate flux calculation
1153 method is not trivial, as different approaches can result in large differences in estimated
1154 flux and have different sensitivities to non-linear patterns of gas concentration within the
1155 chamber, which may arise from both instrument noise and natural processes. On the one
1156 hand, simple linear regression (LM) often underestimates fluxes in non-steady chambers
1157 (Silva et al., 2015), which leads many researchers to default to non-linear (HM) model
1158 (Rheault et al., 2024). However, noisy measurements can lead to the HM model producing
1159 unrealistic fluxes (Hüppi et al., 2018). Additionally, ebullitive dynamics typically force
1160 extreme curvatures of HM and might even cause negative LM flux estimates. To select an
1161 appropriate best-estimate instantaneous flux for every time series, we used sequential
1162 criteria based on the presence of ebullitive patterns and on LM and HM model fit statistics.
1163 This set of criteria was designed to balance the model-specific risks of over- and
1164 underestimation of fluxes, especially for cases with ebullitive patterns, while preserving a
1165 transparent and reproducible approach.

1166 First, all CH₄ timeseries with visual evidence of ebullition (recorded during previous
1167 inspection) were assigned to the two-point flux estimate unless the linear model presented
1168 an R² above 0.99 (LM.r2 > 0.99). For the rest of the timeseries, absent of ebullitive patterns,
1169 the HM model was chosen only when all the following criteria were met (defaulting to the
1170 LM estimate when one or more were violated): HM model produces a valid flux estimate
1171 (HM.flux ≠ NA); LM flux estimate is above the minimal detectable flux (Christiansen et al.,
1172 2015); HM curvature parameter *Kappa* is below the theoretical maximum (Hüppi et al.,
1173 2018); The ratio between the non-linear (HM) flux estimate and the linear (LM) estimate, the
1174 g-fact (Hüppi et al., 2018) is below the gas species-specific custom threshold (CO₂ g-fact <
1175 4; CH₄ g-fact < 3); Akaike Information Criterion corrected for small sample size (AICc) of the
1176 HM model is lower than that of the LM model; Mean absolute error (MAE) of HM model is at
1177 least 5% lower than that of LM model.

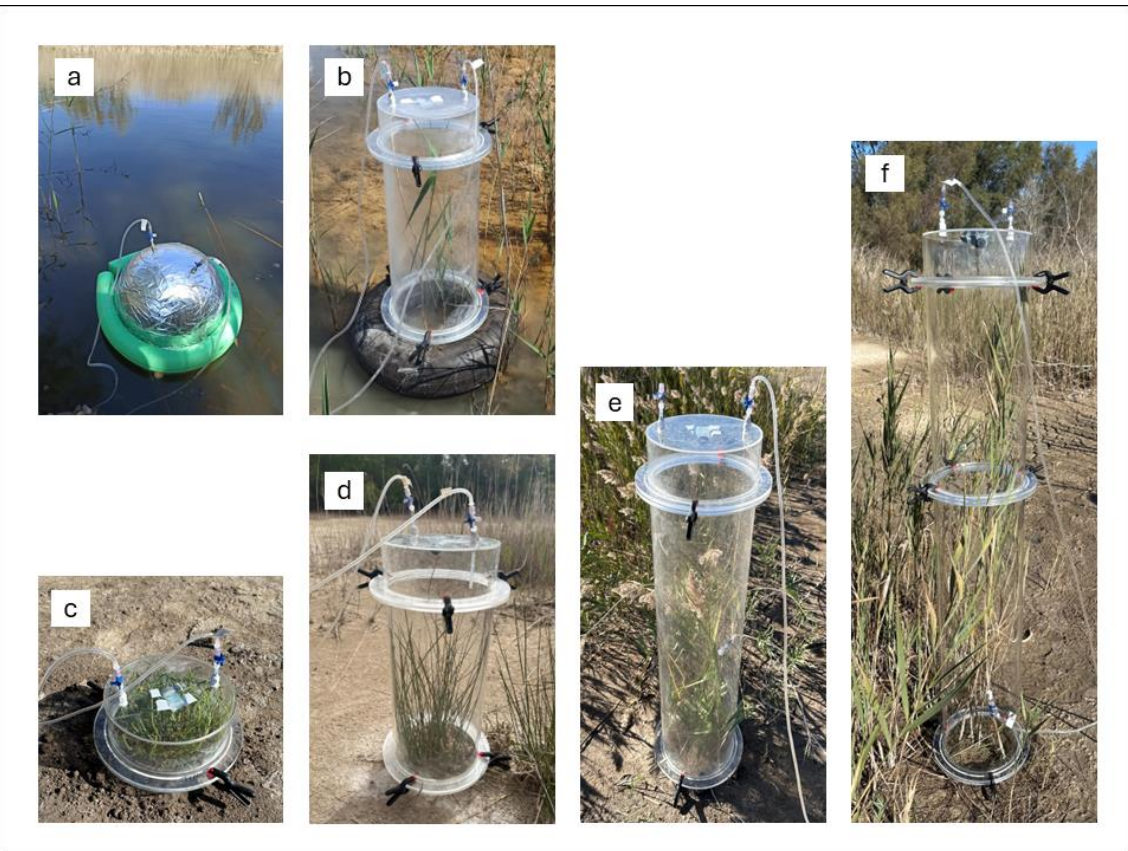
1178 A larger g-fact threshold was allowed for CO₂ time series (compared to CH₄) to account for
1179 cases where CO₂ concentration inside the chamber might cause limitation of
1180 photosynthetic activity and associated attenuation of uptake rate during the incubation.
1181 Using this set of criteria, the chosen best model for CO₂ fluxes was LM for 1914 timeseries

1182 (64%) and HM for 1076 timeseries (36%). For CH₄ fluxes, the best model was two-point for
1183 631 (21.1%), LM for 1850 (62%) and HM for 505 (16.9%) of the time series.

1184 **3. Supplementary Figures**



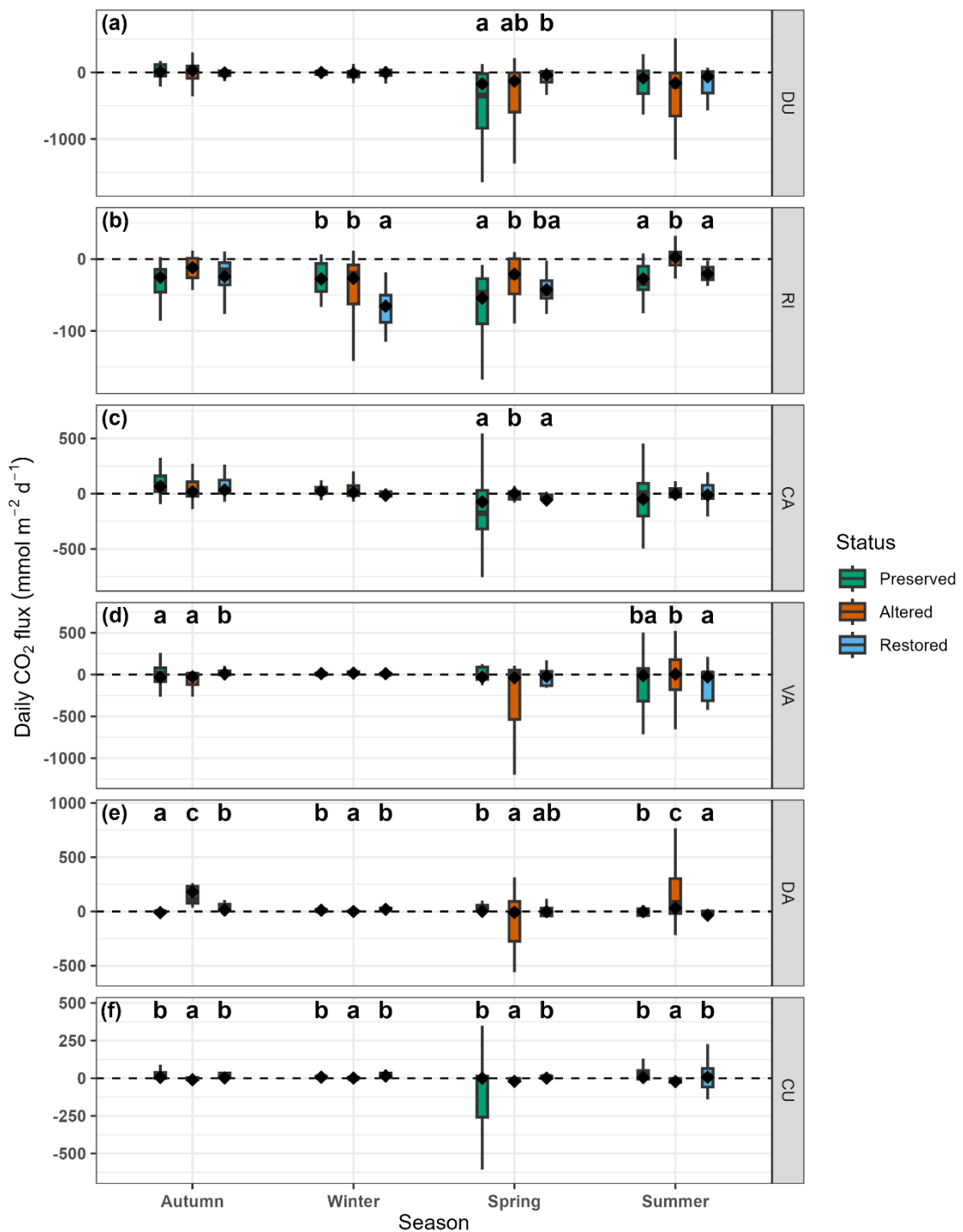
1185
1186 **Figure S1. Representative pictures of case pilot preserved wetlands.** Pictures
1187 depict (a) saltmarsh of South-west Dutch Delta (DU), (b) *Zostera noltii* meadow
1188 during low tide in Ria de Aveiro (RI), (c) freshwater marshes and ponds of Camargue
1189 (CA), (d) brackish marshes of Marjal dels Moros (VA), (e) freshwater lakes with reed
1190 beds of Danube Delta (DA), (f) freshwater littoral with reeds and submerged
1191 vegetation of Curonian Lagoon (CU). Pictures facilitated by LifeWatch ERIC.
1192

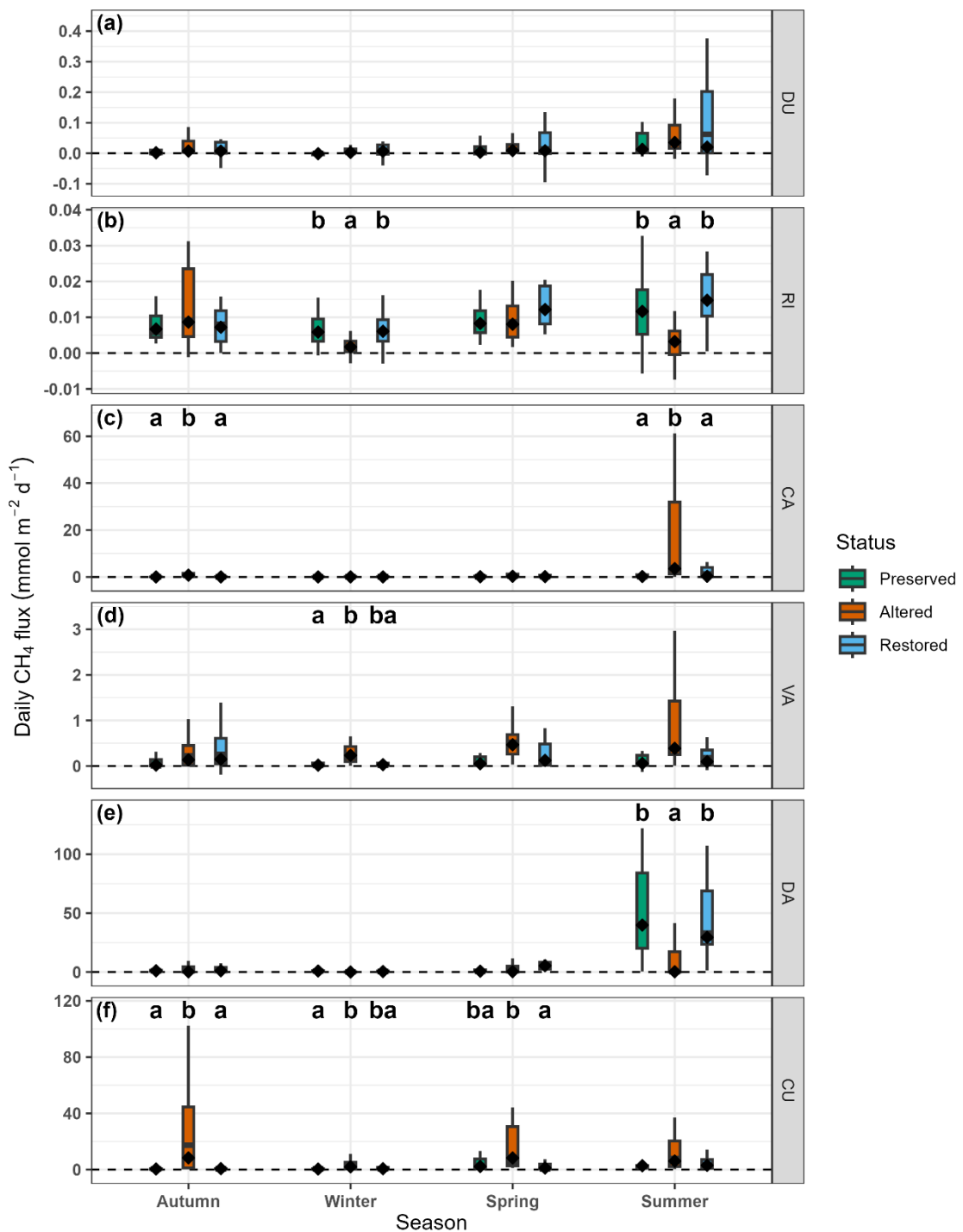


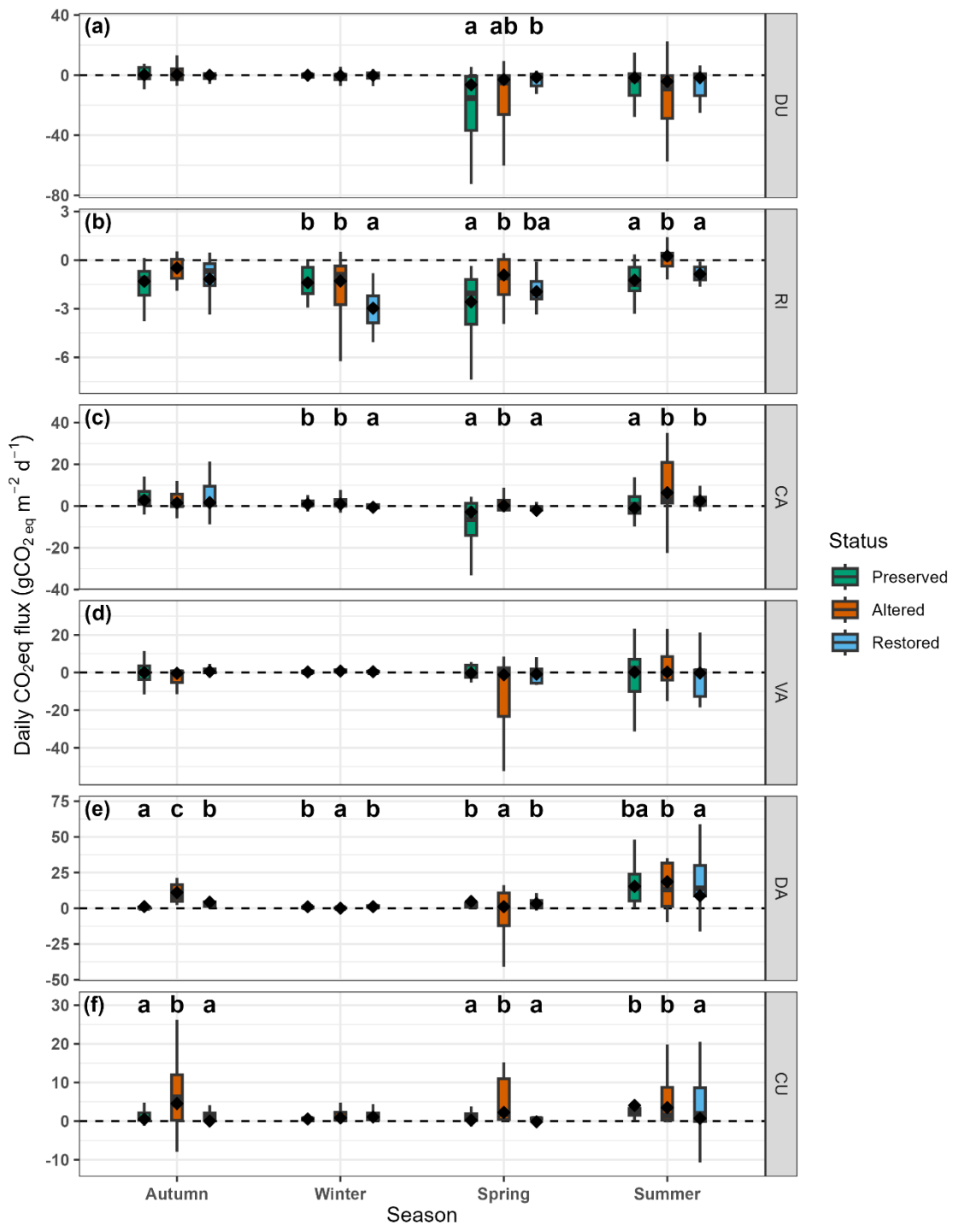
1193

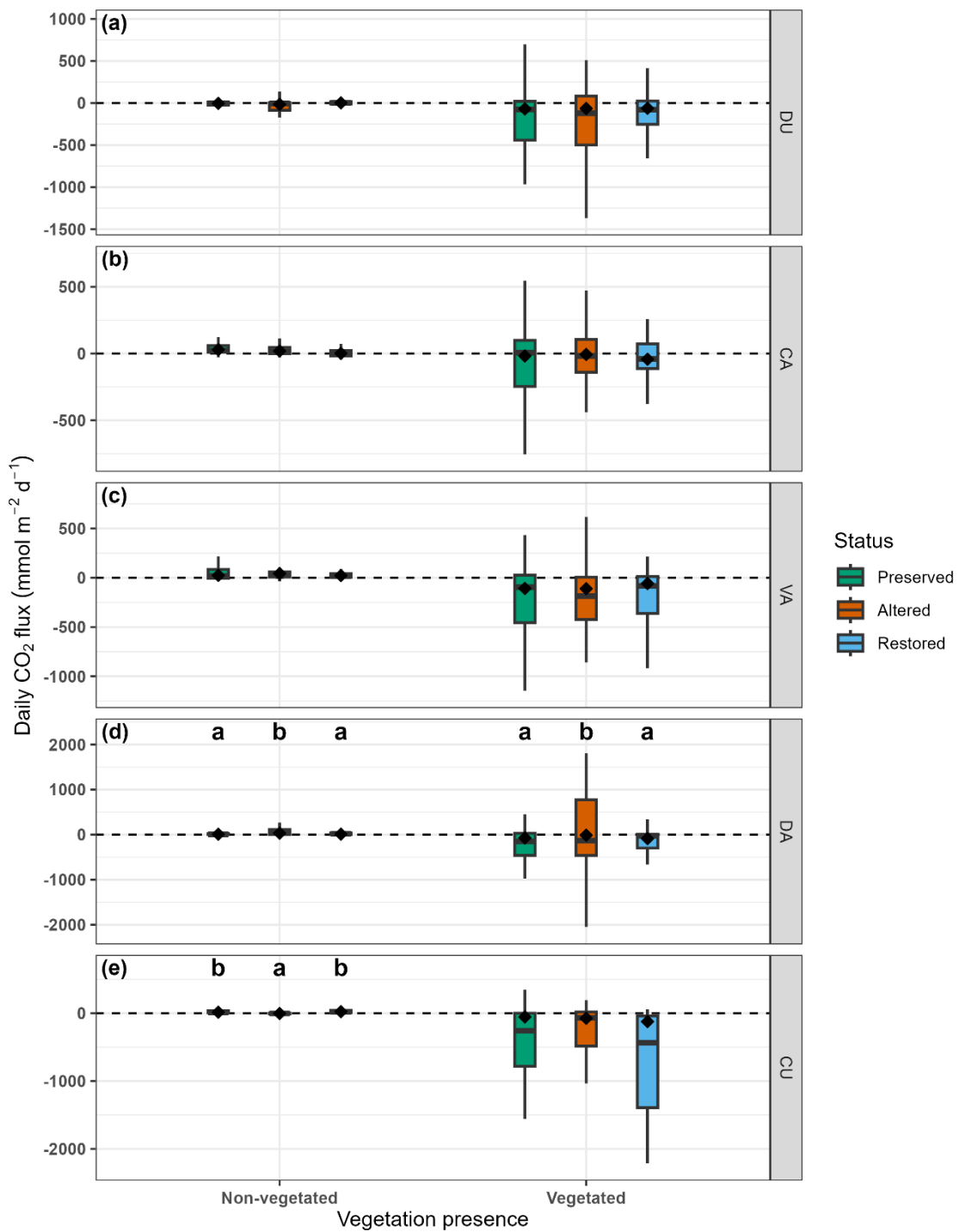
1194 **Figure S2. Static chamber types and configurations.** (a) Opaque semi-spherical
 1195 floating chamber used in open water areas, (b) transparent modular cylindrical
 1196 chamber with floating device used in flooded areas with emergent vegetation, (c-f)
 1197 transparent modular cylindrical chamber used in non-flooded areas in increasing-
 1198 volume configurations. Dark incubations using the cylindrical modular chamber
 1199 involved the use of an opaque textile cover (not shown).

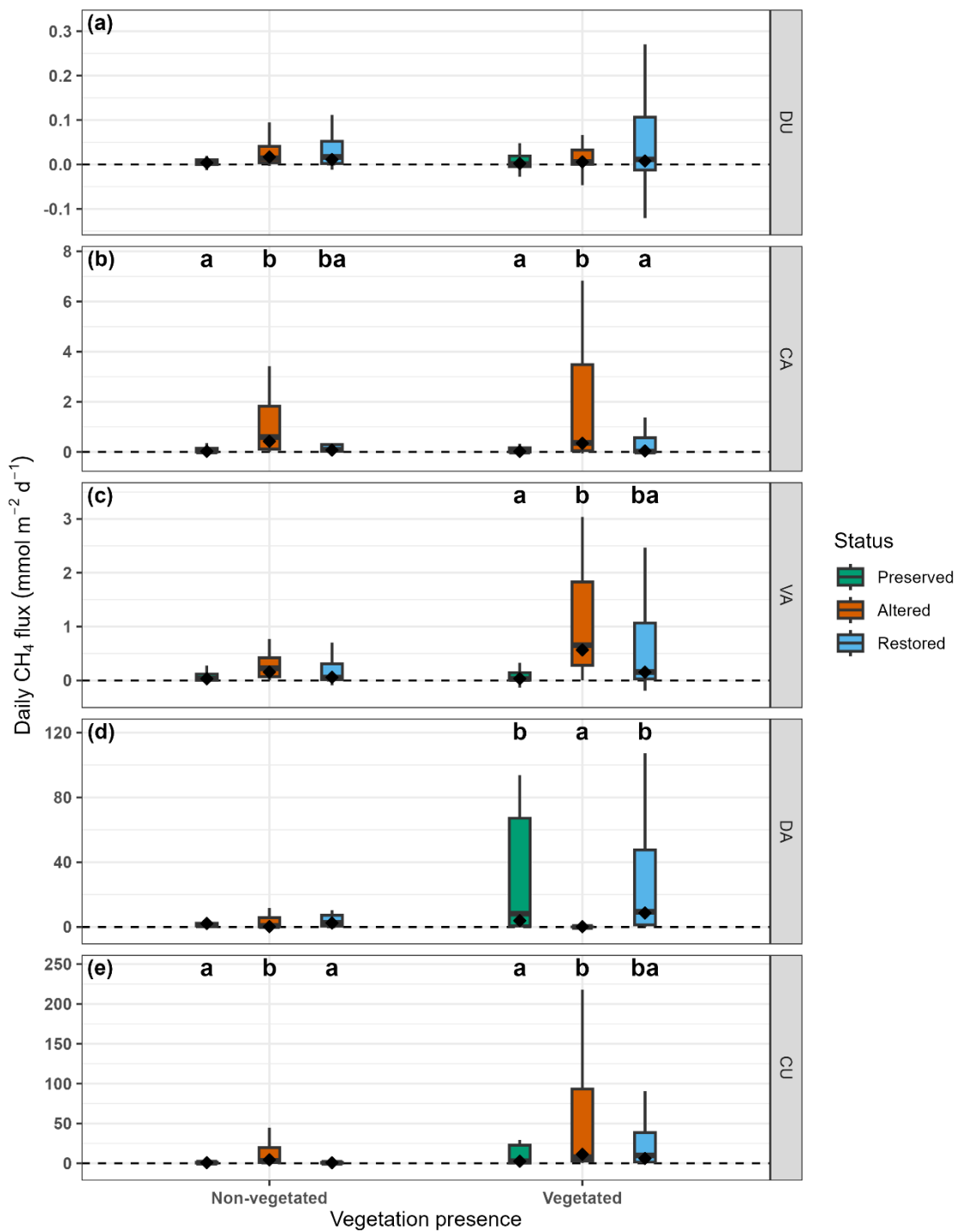
1200

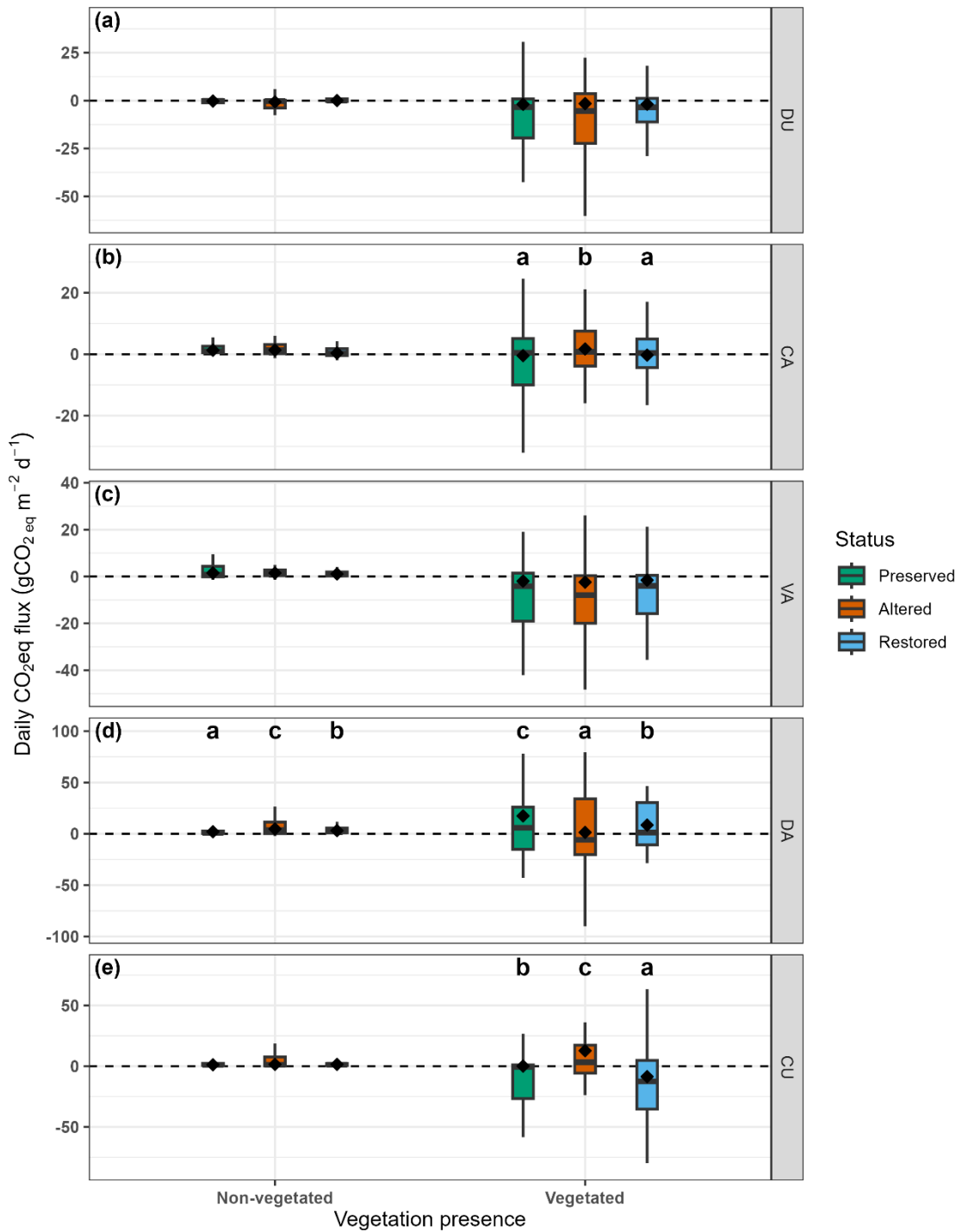












4. Supplementary tables

Table S1. GLMM model summaries. Model structure (formula call, distribution and data transformation), number of samples (N), marginal and conditional R-squared values (R^2m and R^2c) representing the proportion of variance explained by the model and significance of fixed effects (conservation status, season, vegetation presence and interactions) for each case pilot-GHG flux dataset.

Dataset	Best-Supported Model	N	R^2m	R^2c	Effect	p-Value
DU - CO ₂	Call: Flux ~ status * season * vegpresence + (1 site), Distribution: t, Transformation: pseudo-log	349	0.494	0.515	status	0.764
					season	< 0.001
					vegpresence	< 0.001
					status : season	0.011
					status : vegpresence	0.418
					status : season : vegpresence	0.014
RI - CO ₂	Call: Flux ~ status * season + (1 site), Distribution: gaussian, Transformation: pseudo-log	266	0.315	0.347	status	< 0.001
					season	< 0.001
					status : season	0.001
					status	0.268
CA - CO ₂	Call: Flux ~ status * season * vegpresence + (1 site), Distribution: t, Transformation: pseudo-log	346	0.473	0.537	season	< 0.001
					vegpresence	< 0.001
					status : season	< 0.001
					status : vegpresence	0.206
					status : season : vegpresence	< 0.001

Dataset	Best-Supported Model	N	R ² m	R ² c	Effect	p-Value
VA - CO ₂	Call: Flux ~ status * season * vegpresence + (1 site), Distribution: t, Transformation: pseudo-log	340	0.741	0.749	status	0.627
					season	< 0.001
					vegpresence	< 0.001
					status : season	< 0.001
					status : vegpresence	0.001
					status : season : vegpresence	< 0.001
					status	< 0.001
					season	< 0.001
					vegpresence	< 0.001
					status : season	< 0.001
DA - CO ₂	Call: Flux ~ status * season * vegpresence + (1 site), Distribution: t, Transformation: pseudo-log	296	0.800	0.800	status : vegpresence	0.003
					status : season : vegpresence	< 0.001
					status	< 0.001
					season	< 0.001
					vegpresence	< 0.001
					status : season	< 0.001
					status : vegpresence	0.003
					status : season : vegpresence	< 0.001
					status	< 0.001
					season	< 0.001
CU - CO ₂	Call: Flux ~ status * season * vegpresence + (1 site), Distribution: t, Transformation: pseudo-log	320	0.763	0.764	vegpresence	< 0.001
					status : season	< 0.001
					status : vegpresence	< 0.001
					status : season : vegpresence	< 0.001
					status	0.521
					season	< 0.001
					vegpresence	< 0.001
					status : season	< 0.001
					status : vegpresence	< 0.001
					status : season : vegpresence	< 0.001
DU - CH ₄		346	0.141	0.285	status	0.521

Dataset	Best-Supported Model	N	R ² m	R ² c	Effect	p-Value
	Call: Flux ~ status * season * vegpresence + (1 site), Distribution: gaussian, Transformation: pseudo-log				season	< 0.001
					vegpresence	0.02
					status : season	0.715
					status : vegpresence	0.379
					status : season : vegpresence	0.945
RI - CH ₄	Call: Flux ~ status * season + (1 site), Distribution: t, Transformation: pseudo-log	265	0.221	0.225	status	< 0.001
					season	< 0.001
					status : season	< 0.001
CA - CH ₄	Call: Flux ~ status * season * vegpresence + (1 site), Distribution: gaussian, Transformation: pseudo-log	345	0.390	0.436	status	0.001
					season	< 0.001
					vegpresence	0.232
					status : season	< 0.001
					status : vegpresence	0.78
					status : season : vegpresence	0.491
VA - CH ₄	Call: Flux ~ status * season * vegpresence + (1 site), Distribution: gaussian, Transformation: pseudo-log	337	0.262	0.393	status	0.039
					season	0.005
					vegpresence	< 0.001
					status : season	0.057
					status : vegpresence	0.04

Dataset	Best-Supported Model	N	R ² m	R ² c	Effect	p-Value
DA - CH ₄	Call: Flux ~ status * season * vegpresence + (1 site), Distribution: t, Transformation: log	306	0.502	0.678	status : season : vegpresence	0.63
					status	0.011
					season	< 0.001
					vegpresence	0.026
					status : season	< 0.001
					status : vegpresence	0.046
					status : season : vegpresence	< 0.001
					status	0.003
					season	< 0.001
					vegpresence	< 0.001
CU - CH ₄	Call: Flux ~ status * season * vegpresence + (1 site), Distribution: gaussian, Transformation: pseudo-log	317	0.526	0.585	status : season	< 0.001
					status : vegpresence	0.012
					status : season : vegpresence	0.005
					status	0.757
					season	< 0.001
					vegpresence	< 0.001
					status : season	0.211
					status : vegpresence	0.192
					status : season : vegpresence	0.252
DU - CO ₂ -eq	Call: Flux ~ status * season * vegpresence + (1 site), Distribution: gaussian, Transformation: arcsinh	345	0.382	0.393		

Dataset	Best-Supported Model	N	R ² m	R ² c	Effect	p-Value
RI - CO ₂ -eq	Call: Flux ~ status * season + (1 site), Distribution: gaussian, Transformation: Yeo-Johnson	263	0.325	0.343	status	< 0.001
					season	< 0.001
					status : season	0.003
CA - CO ₂ -eq	Call: Flux ~ status * season * vegpresence + (1 site), Distribution: t, Transformation: arcsinh	342	0.489	0.514	status	0.026
					season	< 0.001
					vegpresence	< 0.001
					status : season	< 0.001
					status : vegpresence	0.004
					status : season : vegpresence	< 0.001
					status	0.96
VA - CO ₂ -eq	Call: Flux ~ status * season * vegpresence + (1 site), Distribution: gaussian, Transformation: arcsinh	333	0.527	0.545	season	< 0.001
					vegpresence	< 0.001
					status : season	0.368
					status : vegpresence	0.304
					status : season : vegpresence	0.148
					status	< 0.001
					season	< 0.001
DA - CO ₂ -eq	Call: Flux ~ status * season * vegpresence + (1 site), Distribution: t, Transformation: arcsinh	292	0.718	0.718	vegpresence	< 0.001
					status : season	< 0.001

Dataset	Best-Supported Model	N	R ² m	R ² c	Effect	p-Value
CU - CO ₂ -eq	Call: Flux ~ status * season * vegpresence + (1 site), Distribution: t, Transformation: pseudo-log	312	0.656	0.682	status : vegpresence	< 0.001
					status : season : vegpresence	< 0.001
					status	< 0.001
					season	< 0.001
					vegpresence	< 0.001
					status : season	< 0.001
					status : vegpresence	< 0.001
					status : season : vegpresence	< 0.001

Table S2. Model-derived estimated marginal means (EMMs). EMM, standard error and 95% confidence interval of GHG fluxes (CO₂, CH₄, CO₂-eq) for different conservation status of each case pilot wetland across seasons and vegetation presence.

Case pilot	Status	CO2 flux (mmol m ⁻² d ⁻¹)		CH4 flux (mmol m ⁻² d ⁻¹)		GWP flux (g CO ₂ -eq. m ⁻² d ⁻¹)	
		Mean ± SE	95% CI	Mean ± SE	95% CI	Mean ± SE	95% CI
RI	Preserved	-32.4 ± 5.14	-42.6 to -22.3	0.0079 ± 0.00075	0.00643 to 0.00937	-1.59 ± 0.228	-2.04 to -1.14
	Altered	-13.4 ± 3.44	-20.2 to -6.64	0.00492 ± 0.000564	0.00381 to 0.00602	-0.519 ± 0.148	-0.812 to -0.227
	Restored	-35.4 ± 5.68	-46.6 to -24.2	0.00953 ± 0.000916	0.00773 to 0.0113	-1.65 ± 0.245	-2.13 to -1.17
DU	Preserved	-37.8 ± 13.8	-64.8 to -10.7	0.00272 ± 0.00315	-0.00347 to 0.00892	-1.09 ± 0.346	-1.77 to -0.405
	Altered	-42.1 ± 13.6	-68.8 to -15.4	0.00921 ± 0.00698	-0.00453 to 0.0229	-1.18 ± 0.36	-1.88 to -0.466
	Restored	-26.1 ± 11	-47.7 to -4.63	0.00921 ± 0.00701	-0.00458 to 0.023	-0.765 ± 0.301	-1.36 to -0.172
CA	Preserved	-5.13 ± 10.5	-25.7 to 15.4	0.0237 ± 0.0134	-0.00259 to 0.0501	-0.00711 ± 0.289	-0.574 to 0.56
	Altered	6.1 ± 10.7	-14.9 to 27.1	0.384 ± 0.215	-0.038 to 0.806	1.5 ± 0.58	0.364 to 2.64
	Restored	-9.67 ± 11.2	-31.6 to 12.3	0.0583 ± 0.0328	-0.00627 to 0.123	0.227 ± 0.3	-0.361 to 0.816
VA	Preserved	-13.8 ± 5.95	-25.4 to -2.13	0.0312 ± 0.0197	-0.00763 to 0.07	0.0204 ± 0.254	-0.48 to 0.521
	Altered	-7.98 ± 4.46	-16.7 to 0.755	0.273 ± 0.169	-0.0592 to 0.606	-0.133 ± 0.258	-0.64 to 0.374
	Restored	-6.3 ± 5.02	-16.1 to 3.55	0.0839 ± 0.0521	-0.0186 to 0.186	-0.0359 ± 0.258	-0.543 to 0.471
DA	Preserved	-0.0447 ± 0.844	-1.7 to 1.61	2.38 ± 1.85	-1.25 to 6	3.3 ± 0.241	2.83 to 3.77
	Altered	13.9 ± 1.4	11.2 to 16.6	0.182 ± 0.17	-0.151 to 0.514	3.4 ± 0.267	2.87 to 3.92
	Restored	1.07 ± 1.11	-1.1 to 3.24	3.07 ± 2.4	-1.63 to 7.77	3.56 ± 0.352	2.87 to 4.25
CU	Preserved	4.13 ± 0.801	2.56 to 5.7	0.982 ± 0.339	0.316 to 1.65	0.89 ± 0.293	0.316 to 1.46
	Altered	-8.7 ± 1.36	-11.4 to -6.04	5.32 ± 1.83	1.72 to 8.92	2.41 ± 0.657	1.12 to 3.7
	Restored	5 ± 0.895	3.24 to 6.75	1.07 ± 0.374	0.337 to 1.81	0.346 ± 0.226	-0.098 to 0.789

Table S3. Post-hoc contrasts between model-derived averages (EMMs) of (a) CO₂, (b) CH₄ and (c) CO₂-eq daily fluxes between different conservation status classes of each case pilot. Estimate, standard error, 95% confidence interval and significance (P-value) are provided for each conservation status contrast across seasons. Negative flux differences for Preserved – Altered contrast represent avoided emissions through conservation. Negative flux differences for Restored – Altered contrasts represent mitigated emissions through restoration. Positive flux differences for Restored – Preserved contrasts represent functional recovery debt of restoration. All significance tests were computed in model-scale using t-tests or z-tests (for gaussian or t-family models, respectively) and flux differences were back-transformed according to the dataset-specific transformation function (Table S1).

Table S3a. Daily CO₂ flux contrasts for conservation status across seasons.

Case pilot	Contrast	Daily CO ₂ flux difference (mmol m ⁻² d ⁻¹)		
		Estimate ± SE	95% CI	P-value
DU	Preserved - Altered	4.33 ± 19.4	-33.6 to 42.3	0.994
	Restored - Altered	15.9 ± 17.5	-18.3 to 50.2	0.73
	Restored - Preserved	11.6 ± 17.6	-22.9 to 46.2	0.878
RI	Preserved - Altered	-19 ± 6.19	-31.2 to -6.84	0.004
	Restored - Altered	-22 ± 6.64	-35.1 to -8.93	0.001
	Restored - Preserved	-2.99 ± 7.66	-18.1 to 12.1	0.972
CA	Preserved - Altered	-11.2 ± 15	-40.6 to 18.2	0.831
	Restored - Altered	-15.8 ± 15.5	-46.2 to 14.6	0.65
	Restored - Preserved	-4.54 ± 15.3	-34.6 to 25.5	0.987
VA	Preserved - Altered	-5.81 ± 7.43	-20.4 to 8.75	0.817
	Restored - Altered	1.68 ± 6.71	-11.5 to 14.8	0.992
	Restored - Preserved	7.49 ± 7.78	-7.76 to 22.7	0.703
DA	Preserved - Altered	-13.9 ± 1.63	-17.1 to -10.7	< 0.001
	Restored - Altered	-12.8 ± 1.78	-16.3 to -9.33	< 0.001
	Restored - Preserved	1.11 ± 1.39	-1.61 to 3.84	0.81
CU	Preserved - Altered	12.8 ± 1.58	9.74 to 15.9	< 0.001
	Restored - Altered	13.7 ± 1.63	10.5 to 16.9	< 0.001
	Restored - Preserved	0.862 ± 1.2	-1.49 to 3.22	0.852

Table S3b. Daily CH₄ flux contrasts for conservation status across seasons.

Case pilot	Contrast	Daily CH ₄ flux difference (mmol m ⁻² d ⁻¹)		
		Estimate ± SE	95% CI	P-value
DU	Preserved - Altered	-0.00648 ± 0.00766	-0.0215 to 0.00858	0.699
	Restored - Altered	4.6e-06 ± 0.00989	-0.0195 to 0.0195	1
	Restored - Preserved	0.00649 ± 0.00768	-0.00863 to 0.0216	0.7
RI	Preserved - Altered	0.00299 ± 0.000938	0.00115 to 0.00482	0.004
	Restored - Altered	0.00461 ± 0.00108	0.0025 to 0.00672	< 0.001
	Restored - Preserved	0.00163 ± 0.00118	-0.000694 to 0.00395	0.42
CA	Preserved - Altered	-0.36 ± 0.215	-0.783 to 0.0626	0.002
	Restored - Altered	-0.326 ± 0.217	-0.753 to 0.101	0.053
	Restored - Preserved	0.0345 ± 0.0354	-0.0352 to 0.104	0.596
VA	Preserved - Altered	-0.242 ± 0.17	-0.577 to 0.0926	0.041
	Restored - Altered	-0.19 ± 0.177	-0.538 to 0.159	0.445
	Restored - Preserved	0.0527 ± 0.0557	-0.0569 to 0.162	0.601
DA	Preserved - Altered	2.2 ± 1.86	-1.44 to 5.83	0.08
	Restored - Altered	2.89 ± 2.4	-1.82 to 7.6	0.044
	Restored - Preserved	0.691 ± 3.03	-5.24 to 6.62	0.994
CU	Preserved - Altered	-4.34 ± 1.86	-8 to -0.68	0.002
	Restored - Altered	-4.25 ± 1.87	-7.93 to -0.577	0.004
	Restored - Preserved	0.09 ± 0.504	-0.902 to 1.08	0.997

Table S3b. Daily CO₂-eq flux contrasts for conservation status across seasons.

Case pilot	Contrast	Daily CO ₂ -eq difference (g CO ₂ -eq m ⁻² d ⁻¹)		
		Estimate ± SE	95% CI	P-value
DU	Preserved - Altered	0.0889 ± 0.5	-0.895 to 1.07	0.997
	Restored - Altered	0.41 ± 0.47	-0.515 to 1.33	0.761
	Restored - Preserved	0.321 ± 0.459	-0.582 to 1.22	0.861
RI	Preserved - Altered	-1.07 ± 0.272	-1.61 to -0.538	< 0.001

Case pilot	Contrast	Daily CO ₂ -eq difference (g CO ₂ -eq m ⁻² d ⁻¹)		
		Estimate ± SE	95% CI	P-value
CA	Restored - Altered	-1.13 ± 0.286	-1.69 to -0.566	< 0.001
	Restored - Preserved	-0.0568 ± 0.334	-0.715 to 0.601	0.998
	Preserved - Altered	-1.51 ± 0.648	-2.78 to -0.238	0.018
	Restored - Altered	-1.27 ± 0.653	-2.55 to 0.00645	0.085
	Restored - Preserved	0.234 ± 0.417	-0.583 to 1.05	0.92
	Preserved - Altered	0.153 ± 0.362	-0.559 to 0.866	0.965
VA	Restored - Altered	0.0969 ± 0.364	-0.62 to 0.814	0.991
	Restored - Preserved	-0.0564 ± 0.362	-0.769 to 0.656	0.998
	Preserved - Altered	-0.0967 ± 0.36	-0.802 to 0.608	0.99
DA	Restored - Altered	0.161 ± 0.442	-0.705 to 1.03	0.977
	Restored - Preserved	0.258 ± 0.427	-0.578 to 1.09	0.905
	Preserved - Altered	-1.52 ± 0.719	-2.93 to -0.11	0.046
CU	Restored - Altered	-2.06 ± 0.695	-3.43 to -0.702	< 0.001
	Restored - Preserved	-0.544 ± 0.37	-1.27 to 0.181	0.344

Table S4. Summary of surface water parameters for different conservation status of each case pilot wetland. Chlorophyll-a (Chl-a), electrical conductivity (EC), total nitrogen (Total N) and total phosphorus (Total P) were determined using common analytical techniques (Santinelli et al., submitted). Total nitrogen and phosphorus include both particulate and dissolved nutrients.

Case pilot	Status	N	Chl-a (µg L-1)	EC (mS cm-1)	Total N (µM)	Total P (µM)
			Mean ± SE	Mean ± SE	Mean ± SE	Mean ± SE
DU	Preserved	24	4.40 ± 0.77	22.73 ± 2.57	90.98 ± 13.39	3.85 ± 0.49
	Altered	24	7.17 ± 2.87	24.75 ± 2.40	92.29 ± 15.65	13.01 ± 4.51
	Restored	24	3.66 ± 0.72	23.47 ± 2.64	107.24 ± 14.28	5.53 ± 0.84
RI	Preserved	24	1.66 ± 0.25	32.76 ± 2.60	40.76 ± 4.65	1.38 ± 0.06
	Altered	24	1.76 ± 0.21	26.16 ± 2.90	75.40 ± 9.28	1.62 ± 0.06
	Restored	24	3.18 ± 0.51	25.28 ± 3.31	113.47 ± 19.88	1.77 ± 0.13
CA	Preserved	21	27.56 ± 12.64	9.80 ± 1.17	258.42 ± 20.85	9.02 ± 1.73
	Altered	21	10.41 ± 2.41	3.50 ± 0.68	147.15 ± 19.56	6.23 ± 1.50
	Restored	24	2.21 ± 0.50	1.19 ± 0.10	73.49 ± 9.12	1.49 ± 0.23
VA	Preserved	16	20.77 ± 3.56	84.07 ± 13.21	1513.66 ± 461.66	14.32 ± 9.22
	Altered	24	13.95 ± 3.97	17.67 ± 1.26	286.56 ± 32.97	1.09 ± 0.13
	Restored	21	35.35 ± 9.53	60.16 ± 6.37	703.78 ± 80.30	4.90 ± 0.66
DA	Preserved	24	49.23 ± 10.56	0.52 ± 0.03	137.98 ± 28.56	1.74 ± 0.27
	Altered	12	131.64 ± 45.96	0.66 ± 0.09	290.10 ± 98.31	15.67 ± 4.59
	Restored	24	28.11 ± 6.96	1.40 ± 0.25	237.76 ± 27.71	3.00 ± 0.61
CU	Preserved	24	8.17 ± 1.30	0.53 ± 0.11	124.06 ± 13.90	2.88 ± 0.61
	Altered	24	64.15 ± 7.88	0.32 ± 0.01	217.69 ± 22.22	5.85 ± 0.76
	Restored	24	27.50 ± 4.82	0.32 ± 0.01	137.27 ± 16.38	2.32 0.27

5. Supplementary references

Christiansen, J. R., Outhwaite, J., & Smukler, S. M. (2015). Comparison of CO₂, CH₄ and N₂O soil-atmosphere exchange measured in static chambers with cavity ring-down spectroscopy and gas chromatography. *Agricultural and Forest Meteorology*, 211–212, 48–57. <https://doi.org/10.1016/J.AGRFORMAT.2015.06.004>

Hüppi, R., Felber, R., Krauss, M., Six, J., Leifeld, J., & Fuß, R. (2018). Restricting the nonlinearity parameter in soil greenhouse gas flux calculation for more reliable flux estimates. *PLOS ONE*, 13(7), e0200876. <https://doi.org/10.1371/journal.pone.0200876>

Hutchinson, G. L., & Mosier, A. R. (1981). Improved Soil Cover Method for Field Measurement of Nitrous Oxide Fluxes. *Soil Science Society of America Journal*, 45(2), 311–316. <https://doi.org/10.2136/sssaj1981.03615995004500020017x>

Idzelyte-, R., Cerkasova, N., Mezine-, J., Dabulevičiene-, T., Razinkovas-Baziukas, A., Ertürk, A., & Umgiesser, G. (2023). Coupled hydrological and hydrodynamic modelling application for climate change impact assessment in the Nemunas river watershed-Curonian Lagoon-southeastern Baltic Sea continuum. *Ocean Science*, 19(4), 1047–1066. <https://doi.org/10.5194/OS-19-1047-2023>

Rheault, K., Christiansen, J. R., & Larsen, K. S. (2024). goFlux: A user-friendly way to calculate GHG fluxes yourself, regardless of user experience. *Journal of Open Source Software*, 9(96), 6393. <https://doi.org/10.21105/joss.06393>

Santinelli, C., Rochera, C., Tropea, C., Schiller, J., Adamescu, M., Ambrosio, R., Attermeyer, K., Bachi, G., Bègue, N., Bučas, M., Cabrera-Brufau, M., Camacho-Santamans, A., Carballeira, R., Carloni, M., Cavalcante, L., Cazacu, C., Checcucci, G., Coelho, P., Dinu, V., ... Camacho, A. (n.d.). Hydrological and landscape controls on dissolved organic matter dynamics in European wetlands: Implications for management and restoration. *Submitted to Biogeosciences*.

Silva, J. P., Lasso, A., Lubberding, H. J., Peña, M. R., & Gijzen, H. J. (2015). Biases in greenhouse gases static chambers measurements in stabilization ponds: Comparison of flux estimation using linear and non-linear models. *Atmospheric Environment*, 109, 130–138. <https://doi.org/10.1016/J.ATMOSENV.2015.02.068>

Stakénienė, R., Jokšas, K., Kriauciūnienė, J., Jakimavičius, D., & Raudonytė-Svirbutavičienė, E. (2023). Nutrient Loadings and Exchange between the Curonian Lagoon and the Baltic Sea: Changes over the Past Two Decades (2001–2020). *Water 2023, Vol. 15, Page 4096*, 15(23), 4096. <https://doi.org/10.3390/W15234096>